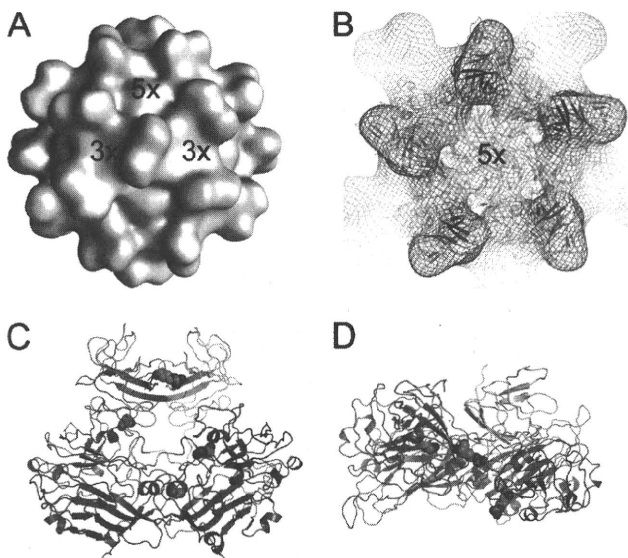

FIG. 4. The structure of the chimeric HEV VLP carrying a B-cell tag. (A) Surface presentation of VLP-C-tag viewed along an icosahedral 2-fold axis. (B) The cryo-EM density map of VLP-C-tag (mesh) was fitted with the crystal structure of the PORF2 decamer (ribbon). (C) Ribbon representation of PORF2 dimer with one monomer colored gray and the other colored pink for the S1 domain, blue for the M domain, and lime for the P domain. The amino acids prior to the four internal insertion sites are marked in sphere mode with color coding representing the elements as described in the Fig. 3 legend. (D) The top view of the PORF2 dimer, showing the location of the non-VLP insertion sites.

B-cell tag of 11 amino acids was incorporated into the C terminus of PORF2 (Fig. 1B). A total of 782 images of individual particles were used to reconstruct the final three-dimensional model of VLP-C-tag. In agreement with the previously published cryo-EM VLP structures, the surface of VLP-C-tag can be divided into two distinct layers, an icosahedral shell and a protruding spike (Fig. 4A). The spike projects outward from the icosahedral shell and is composed of a PORF2 dimer. The distance between two adjacent spikes was ~76 Å as measured between the centers of the surface plateaus. These results are consistent with the measurements of VLPs obtained either from Tn5 insect cells (30) or from Sf9 insect cells (13), and no detectable density was added onto the outer surface of the spike. No RNA density was detected within the chimeric VLP-C-tag.

The crystal structure fit very well within the VLP-C-tag density map (Fig. 4B), indicating that the insertion of the C-terminal 11 amino acids inhibits neither the dimer-dimer interactions nor the formation of T=1 VLP. When the density maps were contoured to cover 100%, the radii of the S domains were roughly the same for both the VLP-C-tag and the VLP-Fab224 map, and the heights of the protruding spikes appeared similar. No density difference was observed from the docking (Fig. 5), suggesting that the inserted B-cell tag is flexible and less ordered. However, model fitting revealed that coordinates with unoccupied density appeared at the lateral side of the spike and underneath the Fab224 binding site (Fig. 5A and B), which may correspond to the inserted peptide.

DISCUSSION

HEV T=1 VLP is a vaccine candidate that induces protective immunity in nonhuman primates (12). It can also be used as an antigen carrier to deliver foreign epitopes through oral administration (20). Therefore, structural analysis of the antibody recognition sites is essential to suppress the neutralization effect of host vector-specific antibodies. For this purpose, we determined the structure of HEV VLP in complex with antibodies Fab224 (VLP-Fab224) and Fab4 (VLP-Fab4) and the structure of chimeric HEV VLP carrying a B-cell tag at the C terminus of PORF2 (VLP-C-tag). Docking the PORF2 crys-

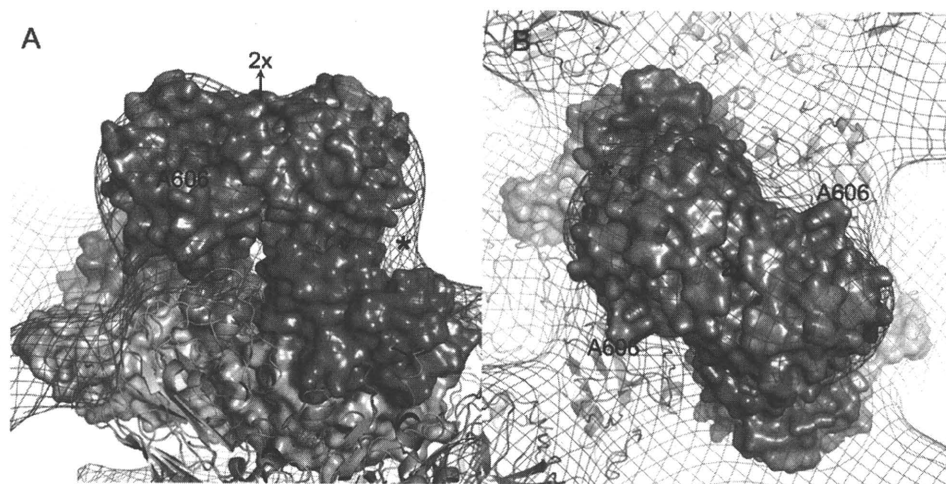

FIG. 5. Fitting of the PORF2 structure into the cryo-EM density map of HEV VLP-C-tag. The side view (A) and the top view (B) of the fitted PORF2 dimer (surface presentation) are overlapped with the cryo-EM density map of VLP-C-tag (mesh). The C-terminal residue A606 is located at the side of the protruding spike. One PORF2 dimer in the surface presentation is colored light magenta, blue violet, and gray for the S, M, and P domain, respectively. The ribbon representation shows the adjacent dimers. The amino acids in PORF2 responsible for binding to Fab224 are colored green for carbon, blue for nitrogen, and red for oxygen. Asterisks mark the location of the extra density that was not occupied with PORF2 coordinates.

tal structure provides spatial information on the HEV antigenic domain and structural guidance to better design foreign epitope insertion.

Structure of the neutralization epitopes. The antigenic properties of HEV and the mechanisms by which it is neutralized are difficult to characterize due to the lack of adequate cell culture replication systems. Therefore, our understanding of HEV immunology is mainly based on studies using recombinant proteins expressed in *E. coli* (23) and recombinant proteins or HEV VLPs generated using the baculovirus expression systems (15, 24). Data from these studies indicate that the C-terminal region of PORF2 participates in the immune response against HEV and that the HEV neutralization epitope is conformational. The minimum peptide required to induce HEV-neutralizing antibodies corresponds to a region of 148 residues in PORF2, from amino acids 459 to 607 (33). This peptide coincides with the P domain revealed in the crystal structures of PORF2. The density of the Fab in our cryo-EM structure interfaced entirely with the spikes, thus confirming that the P domain is primarily responsible for HEV antigenicity. Fab4 is a chimpanzee antibody that recognizes the ORF2 protein and was isolated from a cDNA library by using phage display (25). Fab4 binds to native HEV virions and recombinant PORF2 peptides containing amino acids 597 to 607 (26). We performed fitting with the VLP-Fab4 structure; however, the Fab4 density was too weak to conclusively determine the Fab4 binding site on the surface of HEV VLP. However, the density corresponding to the Fab4 molecule did cover amino acid 606 (data not shown). It is not clear why Fab224 appeared not to interact with peptides lacking amino acids 599 to 608 in immunoblot analysis. However, the Fab224 binding site is consistent with the critical antigenic residues determined previously using mutagenesis. It was found that double mutations that changed residues E479 and K534 or Y485 and I529 to alanine selectively abrogated PORF2's reactivity with neutralizing antibodies (11). Experiments with another set of mutants defined the same region as the HEV antigenic domain, with antibody recognition residues spreading over the AB, CD, and EF loops (32). The antibodies used in both experiments were neutralizing antibodies; therefore, the Fab224 binding surface is part of the dominant neutralization site, suggesting that the monoclonal antibody Fab224 is a neutralizing antibody. This neutralization site partially overlaps with the receptor binding site (32), and antibody binding may create spatial hindrance that prevents HEV VLPs from attaching to the cell surface.

Insertion sites for foreign epitopes. Because they are highly organized capsids that mimic the overall structure of virus particles, VLPs are a robust means by which to simultaneously carry small molecules, peptide antigenic epitopes, and DNA vaccines from heterogeneous sources to target disease sites. However, this rational vaccine design relies on excellent VLP structural information so that epitopes can be effectively conjugated to the VLP surface. In a previous study, rather than selecting PORF2 insertion sites on the basis of structural information, six insertion sites were selected according to restriction enzyme sites located either internally (four sites) or in the N or C terminus of PORF2. The internal sites are located after residues A179, R366, A507, and R542. Fusion proteins carrying insertions at sites A179 and R336 completely failed to produce VLPs, and insertions at A507 and R542 greatly reduced VLP production (20). Crystal structure data revealed that the spatial position of these sites is disadvantageous. Residue A179 is located in the S domain in the middle of an α-helix, which is necessary for the integrity of the S domain and its interaction with the 2-fold-related neighboring subunit. R366 is located in the M domain and favors electrostatic interaction with residue E386 from the 3-fold-related neighboring subunit. Although located within the P domain, the side chain of R542 is within the dimeric interface and guides the hydrophobic interaction of the two monomers. Replacement of R542 may misalign the orientation between two P domains and weaken the dimeric interaction between PORF2 proteins. Residue A507 in the P domain plays an important role in maintaining P domain orientation by fixing the angle of the long proline-rich hinge. Moreover, none of the four residues are exposed on the surface of VLPs, although some of them are located on the surface of individual PORF2 subunits (Fig. 4C and D). Therefore, the insertion of a foreign sequence at these sites does not interfere with the expression of individual proteins but, rather, hinders the assembly of HEV VLPs. The crystal structure revealed that the C terminus is exposed on the surface of VLPs, while the N terminus points toward the VLP center. Therefore, insertion at these two sites does not inhibit VLP assembly; however, the C terminus is more suitable for tethering bulky foreign antigenic sequences, as was shown in a previous report (20).

The cryo-EM structure of the chimeric HEV VLP-C-tag suggested that the B-cell tag was located at the lateral side of the spike, not far from residue A606 (C-terminal end in the crystal structure) (Fig. 5A). This density is located beneath the Fab224 binding site but nonetheless overlaps with the potential binding site of Fab4. As a result, the insertion of the 11-amino-acid B-cell sequence may leave the HEV antigenic site partially open and accessible to the host immune system. This explains why mice can develop antibodies against both HEV and the foreign epitope after oral administration of VLP-C-tag (20).

In conclusion, the cryo-EM structures of VLP-Fab224 identified the lateral surface of the P domain as the recognition site for anti-HEV neutralizing antibodies. The insertion of a B-cell epitope at the PORF2 C terminus does not interfere with T=1 VLP assembly. Thus, T=1 HEV VLPs are a novel tool for oral vaccine delivery, as they constitute nonreplicating entities that can induce mucosal immunity without adjuvant. The induction of antibodies against both HEV and the target disease is an additional advantage of this delivery system.

ACKNOWLEDGMENTS

We thank K. Kato for assistance with antibody preparation and N. Miyazaki for initial model fitting of the P domain structural density.

This project was supported in part by grants from the STINT Foundation, the Medical Research Council, and the PIOMS Institutional Program to R.H.C. This study was also partly funded by a grant from the Swedish Research Council to L.X. J.C.W. and L.X. were supported by grants from the Cancer Research and Discovery Programs, respectively. J.C.W. was initially supported by a grant from NSC as an exchange student under the cosupervision of D. M. Liou and Y. J. Sung.

REFERENCES

1. **Adler, B., and S. Faine.** 1983. A pomona serogroup-specific, agglutinating antigen in Leptospira, identified by monoclonal antibodies. Pathology **15:** 247–250.

2. **Baker, T., and H. Cheng.** 1996. A model based approach for determining orientations of biological macromolecules imaged by cryo-electron microscopy. J. Struct. Biol. **116:**120–130.
3. **Bendall, R. P., V. Ellis, S. Ijaz, P. Thurairajah, and H. R. Dalton.** 2008. Serological response to hepatitis E virus genotype 3 infection: IgG quantitation, avidity, and IgM response. J. Med. Virol. **80:**95–101.
4. **Crowther, R. A.** 1971. Procedures for three-dimensional reconstruction of spherical viruses by Fourier synthesis from electron micrographs. Philos. Trans. R. Soc. Lond. B Biol. Sci. **261:**221–230.
5. **DeLano, W. L.** 2002. The PYMOL molecular graphics system. DeLano Scientific, Palo Alto, CA.
6. **Deshmukh, T. M., K. S. Lole, A. S. Tripathy, and V. A. Arankalle.** 2007. Immunogenicity of candidate hepatitis E virus DNA vaccine expressing complete and truncated ORF2 in mice. Vaccine **25:**4350–4360.
7. **Emerson, S., P. Clemente-Casares, N. Moiduddin, V. A. Arankalle, U. Torian, and R. Purcell.** 2006. Putative neutralization epitopes and broad cross-genotype neutralization of hepatitis E virus confirmed by a quantitative cell-culture assay. J. Gen. Virol. **87:**697–704.
8. **Guu, T., Z. Liu, Q. Ye, D. Mata, K. Li, C. Yin, J. Zhang, and Y. Tao.** 2009. Structure of the hepatitis E virus-like particle suggests mechanisms for virus assembly and receptor binding. Proc. Natl. Acad. Sci. U. S. A. **106:**12992–12997.
9. **Jones, T. A., J. Y. Zou, S. W. Cowan, and M. Kjeldgaard.** 1991. Improved method for building protein models in electron density maps and the location of errors in these models. Acta Crystallogr. A **47**(Pt. 2)**:**110–119.
10. **Khuroo, M. S., and M. S. Khuroo.** 2008. Hepatitis E virus. Curr. Opin. Infect. Dis. **21:**539–543.
11. **Li, S., S. Tang, J. Seetharaman, C. Y. Yang, Y. Gu, J. Zhang, H. Du, J. W. Shih, C. L. Hew, J. Sivaraman, and N. S. Xia.** 2009. Dimerization of hepatitis E virus capsid protein E2s domain is essential for virus-host interaction. PLoS Pathog. **5:**e1000537.
12. **Li, T.-C., Y. Suzaki, Y. Ami, T. N. Dhole, T. Miyamura, and N. Takeda.** 2004. Protection of cynomolgus monkeys against HEV infection by oral administration of recombinant hepatitis E virus-like particles. Vaccine **22:**370–377.
13. **Li, T.-C., N. Takeda, T. Miyamura, Y. Matsuura, J. C. Y. Wang, H. Engvall, L. Hammar, L. Xing, and R. H. Cheng.** 2005. Essential elements of the capsid protein for self-assembly into empty virus-like particles of hepatitis E virus. J. Virol. **79:**12999–13006.
14. **Li, T., N. Takeda, and T. Miyamura.** 2001. Oral administration of hepatitis E virus-like particles induces a systemic and mucosal immune response in mice. Vaccine **19:**3476–3484.
15. **Li, T. C., Y. Yamakawa, K. Suzuki, M. Tatsumi, M. A. Razak, T. Uchida, N. Takeda, and T. Miyamura.** 1997. Expression and self-assembly of empty virus-like particles of hepatitis E virus. J. Virol. **71:**7207–7213.
16. **Maloney, B. J., N. Takeda, Y. Suzaki, Y. Ami, T. C. Li, T. Miyamura, C. J. Arntzen, and H. S. Mason.** 2005. Challenges in creating a vaccine to prevent hepatitis E. Vaccine **23:**1870–1874.
17. **Minuk, G. Y., A. Sun, D. F. Sun, J. Uhanova, L. E. Nicolle, B. Larke, and A. Giulivi.** 2007. Serological evidence of hepatitis E virus infection in an indigenous North American population. Can J. Gastroenterol. **21:**439–442.
18. **Mushahwar, I. K.** 2008. Hepatitis E virus: molecular virology, clinical features, diagnosis, transmission, epidemiology, and prevention. J. Med. Virol. **80:**646–658.
19. **Naik, S. R., R. Aggarwal, P. N. Salunke, and N. N. Mehrotra.** 1992. A large waterborne viral hepatitis E epidemic in Kanpur, India. Bull. World Health Organ. **70:**597–604.
20. **Niikura, M., S. Takamura, G. Kim, S. Kawai, M. Saijo, S. Morikawa, I. Kurane, T. C. Li, N. Takeda, and Y. Yasutomi.** 2002. Chimeric recombinant hepatitis E virus-like particles as an oral vaccine vehicle presenting foreign epitopes. Virology **293:**273–280.
21. **Pavio, N., and J. M. Mansuy.** 2010. Hepatitis E in high-income countries. Curr. Opin. Infect. Dis. **23:**521–527.
22. **Pettersen, E. F., T. D. Goddard, C. C. Huang, G. S. Couch, D. M. Greenblatt, E. C. Meng, and T. E. Ferrin.** 2004. UCSF Chimera—a visualization system for exploratory research and analysis. J. Comput. Chem. **25:**1605–1612.
23. **Riddell, M. A., F. Li, and D. A. Anderson.** 2000. Identification of immunodominant and conformational epitopes in the capsid protein of hepatitis E virus by using monoclonal antibodies. J. Virol. **74:**8011–8017.
24. **Robinson, R. A., W. H. Burgess, S. U. Emerson, R. S. Leibowitz, S. A. Sosnovtseva, S. Tsarev, and R. H. Purcell.** 1998. Structural characterization of recombinant hepatitis E virus ORF2 proteins in baculovirus-infected insect cells. Protein Expr. Purif. **12:**75–84.
25. **Schofield, D. J., J. Glamann, S. U. Emerson, and R. H. Purcell.** 2000. Identification by phage display and characterization of two neutralizing chimpanzee monoclonal antibodies to the hepatitis E virus capsid protein. J. Virol. **74:**5548–5555.
26. **Schofield, D. J., R. H. Purcell, H. T. Nguyen, and S. U. Emerson.** 2003. Monoclonal antibodies that neutralize HEV recognize an antigenic site at the carboxyterminus of an ORF2 protein vaccine. Vaccine **22:**257–267.
27. **Tsarev, S. A., T. S. Tsareva, S. U. Emerson, S. Govindarajan, M. Shapiro, J. L. Gerin, and R. H. Purcell.** 1997. Recombinant vaccine against hepatitis E: dose response and protection against heterologous challenge. Vaccine **15:**1834–1838.
28. **Worm, H. C., and G. Wirnsberger.** 2004. Hepatitis E vaccines: progress and prospects. Drugs **64:**1517–1531.
29. **Xiao, C., and M. G. Rossmann.** 2007. Interpretation of electron density with stereographic roadmap projections. J. Struct. Biol. **158:**181–186.
30. **Xing, L., K. Kato, T. Li, N. Takeda, T. Miyamura, L. Hammar, and R. H. Cheng.** 1999. Recombinant hepatitis E capsid protein self-assembles into a dual-domain T=1 particle presenting native virus epitopes. Virology **265:**35–45.
31. **Xing, L., T. C. Li, N. Miyazaki, M. N. Simon, J. S. Wall, M. Moore, C. Y. Wang, N. Takeda, T. Wakita, T. Miyamura, and R. H. Cheng.** 2010. Structure of hepatitis E virion-sized particle reveals an RNA-dependent viral assembly pathway. J. Biol. Chem. **285:**33175–33183.
32. **Yamashita, T., Y. Mori, N. Miyazaki, H. Cheng, M. Yoshimura, H. Unno, R. Shima, K. Moriishi, T. Tsukihara, T. C. Li, N. Takeda, T. Miyamura, and Y. Matsuura.** 2009. Biological and immunological characteristics of hepatitis E virus-like particles based on the crystal structure. Proc. Natl. Acad. Sci. U. S. A. **106:**12986–12991.
33. **Zhou, Y. H., R. Purcell, and S. Emerson.** 2005. A truncated ORF2 protein contains the most immunogenic site on ORF2: antibody responses to non-vaccine sequences following challenge of vaccinated and nonvaccinated macaques with hepatitis E virus. Vaccine **23:**3157–3165.

HUMAN GENE THERAPY 22:35–43 (January 2011)
© Mary Ann Liebert, Inc.
DOI: 10.1089/hum.2010.001

Acquisition of HIV-1 Resistance in T Lymphocytes Using an ACA-Specific *E. coli* mRNA Interferase

Hideto Chono,[1,2] Kazuya Matsumoto,[1] Hiroshi Tsuda,[1,2] Naoki Saito,[1,2] Karim Lee,[3] Sujeong Kim,[4] Hiroaki Shibata,[5] Naohide Ageyama,[5] Keiji Terao,[5] Yasuhiro Yasutomi,[5] Junichi Mineno,[1] Sunyoung Kim,[3] Masayori Inouye,[6] and Ikunoshin Kato[1,2]

Abstract

Transcriptional activation of gene expression directed by the long terminal repeat (LTR) of HIV-1 requires both the transactivation response element (TAR) and Tat protein. HIV-1 mutants lacking a functional *tat* gene are not able to proliferate. Here we take a genetic approach to suppress HIV-1 replication based on Tat-dependent production of MazF, an ACA-specific endoribonuclease (mRNA interferase) from *Escherichia coli*. When induced, MazF is known to cause Bak- and NBK-dependent apoptotic cell death in mammalian cells. We first constructed a retroviral vector, in which the *mazF* (ACA-less) gene was inserted under the control of the HIV-1 LTR, which was then transduced into CD4+ T-lymphoid CEM-SS cells in such a way that, upon HIV-1 infection, the *mazF* gene is induced to destroy the infecting HIV-1 mRNA, preventing HIV-1 replication. Indeed, when the transduced cells were infected with HIV-1 IIIB, the viral replication was effectively inhibited, as HIV-1 IIIB p24 could not be detected in the culture medium. Consistently, not only cell growth but also the CD4 level was not affected by the infection. These results suggest that the HIV-1-LTR-regulated *mazF* gene was effectively induced upon HIV-1 IIIB infection, which is sufficient enough to destroy the viral mRNA from the infected HIV-1 IIIB to completely block viral proliferation in the cells, but not to affect normal cell growth. These results indicate that the T cells transduced with the HIV-1-LTR-regulated *mazF* gene acquire HIV-1 resistance, providing an intriguing potential for the use of the HIV-1-LTR-regulated *mazF* gene in anti-HIV gene therapy.

Introduction

RNASE-BASED STRATEGIES for anti-human immunodeficiency virus (HIV) gene therapy may be superior to RNA-based (antisense, ribozyme, or siRNAs) strategies, because the former strategies evade the effects of frequent resistant mutations in HIV-1. MazF is a unique sequence-specific endoribonuclease, or mRNA interferase, encoded by the *Escherichia coli* genome (Zhang *et al.*, 2003). It cleaves mRNA at ACA-specific sequences and effectively inhibits protein synthesis. To date, a number of MazF homologues have been found in various bacteria. These homologues have a wide range of sequence specificities and cleave three- to five-nucleotide RNA sequences in transcripts that play diverse roles in bacterial physiology (Zhu *et al.*, 2006, Yamaguchi and Inouye, 2009), including cell-growth regulation, specific gene regulation (Zhu *et al.*, 2009), and obligatory programmed cell death (Nariya and Inouye, 2008). Induction of *E. coli* MazF mRNA interferase in mammalian cells has been demonstrated to effectively induce Bak- and NBK-dependent apoptotic cell death (Shimazu *et al.*, 2007), indicating that MazF mRNA interferase may be a new and effective tool for gene therapy.

In the HIV-1 life cycle immediately after HIV-1 infection, Tat (transactivator of transcription), an early regulatory protein encoded by the HIV-1 genome, is produced, which subsequently binds to the TAR (transactivation response) sequence to induce the transcription of the HIV-1 genome leading to the expression of other HIV-1 proteins (Berkhout *et al.*, 1989). Therefore, for prevention of HIV-1 infection, it would be a best strategy to preferentially destroy the HIV-1 transcript upon HIV-1 infection. For this purpose, we constructed a Tat-dependent MazF expression system in a

[1]Center for Cell and Gene Therapy, Takara Bio Inc., Otsu, Shiga, 520-2193, Japan.
[2]Biotechnology Research Laboratories, Takara Bio Inc., Otsu, Shiga, 520-2193, Japan.
[3]Department of Biological Sciences, Seoul National University, Seoul 151-742, Korea.
[4]ViroMed Co. Ltd., Seoul 151-818, Korea.
[5]Tsukuba Primate Research Center, National Institute of Biomedical Innovation, Tsukuba, Ibaraki, 305-0843, Japan.
[6]Department of Biochemistry, Robert Wood Johnson Medical School, Piscataway, NJ 08854, USA.

retroviral vector, in which the *mazF* gene was fused downstream of the TAR sequence. As the *E. coli mazF* open-reading frame contains nine ACA sequences, all of them were engineered to MazF-uncleavable sequences without changing the amino acid sequence of MazF. This vector was then transduced into T cells so that MazF production is expected to be induced upon HIV-1 infection. Note that Tat protein produced upon HIV-1 infection induces not only the transcription of infected HIV-1, but also the transcription of the HIV-1 long terminal repeat (LTR)-regulated *mazF* (ACA-less) gene integrated into the genome of the T cells. In the present article, CD4+ T lymphoid line CEM-SS cells were used as T cells, which were transduced with the retroviral vector containing the Tat-inducible *mazF* (ACA-less) gene under the HIV-1-LTR promoter. When the transduced cells were infected with HIV-1 IIIB, the replication of the infected virus was effectively inhibited without affecting cell growth. Notably, the CD4 level after HIV-1 IIIB infection was not affected either. These results suggest that the HIV-1-LTR-regulated *mazF* (ACA-less) gene was effectively induced upon HIV-1 IIIB infection, which is sufficient enough to destroy the viral mRNA from the infected HIV-1 IIIB to completely block viral proliferation in the cells. However, the level of MazF induced is not enough to cause any serious cellular damage, thus maintaining normal cell growth and the CD4 level. These results suggest an intriguing potential for the use of the HIV-1-LTR-regulated *mazF* (ACA-less) gene in anti-HIV gene therapy.

Materials and Methods

Cell lines

293T (ATCC no. CRL-11268) cells were cultured in Dulbecco's modified Eagle medium (DMEM; Sigma-Aldrich, Steinheim, Germany) supplemented with 10% (v/v) fetal bovine serum (FBS; Invitrogen, Carlsbad, CA). CEM-SS cells (Kim *et al.*, 1989) were cultured in RPMI-1640 (Sigma-Aldrich) containing 10% (v/v) FBS (Invitrogen). The doubling time of the cells for each culture condition was calculated by linear regression analysis using Microsoft Excel software (Microsoft, Seattle, WA).

Retroviral vectors

The self-inactivating retroviral vector pMTD3 was constructed by deleting a segment consisting of 267 nucleotides from the 3′LTR U3 region of pMT (Lee *et al.*, 2004). An ACA-less *mazF* gene was synthesized by engineering all nine ACA sequences in the original *E. coli mazF* gene to MazF-uncleavable sequences without changing the amino acid sequence of MazF. The HIV-LTR fragment was obtained from pQBI-LTRgagGFP (Quantum Biotechnologies Inc., Montreal, QC, Canada). To minimize the HIV-LTR sequence, U3-TAR fragments were obtained by PCR. The ACA-less *mazF* gene was inserted downstream of U3-TAR to obtain the final self-inactivating retroviral vector plasmid, pMTD3-U3TAR-MazF. As a control, the green fluorescent protein (GFP) gene was inserted into the vector to obtain pMTD3-U3TAR-GFP.

To mimic HIV replication, two kinds of retroviral vectors that express the HIV-1 Tat protein were constructed as follows: (1) Constitutitve Tat expression system from MLV-LTR. The HIV-1 *tat* gene was synthesized and inserted at the multiple-cloning site of pMT. To easily monitor the gene expression in transduced cells, an internal ribosome entry site (IRES) and a coding region for a fluorescent protein, ZsGreen, were fused downstream of the *tat* gene. Thus, the resulting plasmid, pM-LTR-Tat-ZG, expresses Tat as well as ZsGreen from MLV-LTR. (2) Tat expression system from the HIV-1 LTR. The HIV-LTR-*tat*-polyA cassette was inserted in the opposite direction of pMT, and the ZsGreen marker gene was expressed from a phosphoglycerate kinase (PGK) promoter in the normal orientation of pMT. The resulting vector plasmid was designated as pH-LTR-Tat-ZG.

To enhance the viral titer for efficient *mazF* gene transduction, the HIV-LTR-MazF-polyA cassette was introduced in the opposite direction of the MoMLV-LTR at the multicloning site of pMT plasmid (Lee *et al.*, 2004). A truncated form of the human low-affinity nerve growth factor gene (ΔLNGFR) (Verzeletti *et al.*, 1998) was also introduced into the retrovirus vector as a surface marker. The ΔLNGFR gene is under the control of human PGK promoter. The resultant vector plasmid was designated as pMT-MFR-PL2 (Fig. 1B).

Preparation of retroviral vectors

The self-inactivating retroviral vector was generated by the transient transfection method as follows: The GALV-*env* expression vector plasmid, pVM-GeR, was constructed by replacing the amphotropic-*env* gene of pVM-AE (Yu *et al.*, 2003) with the gibbon ape leukemia virus envelope gene. The GALV-env retroviral vector was produced by co-transfecting 293T cells with the retroviral *gag-pol* expression vector plasmid, pVM-GP (Yu *et al.*, 2003), pVM-GeR, and the self-inactivating retroviral vector plasmid. Two days after transfection, viral supernatant was harvested by filtration of the culture fluid from 293T cells with use of a 0.45-μm filter.

GALV-enveloped retroviral Tat expression vectors and MazF expression vector were also generated as follows: Ecotropic retroviral vectors were generated by the transient transfection method using the packaging plasmids pGP (MLV-*gag-pol*; Takara Bio, Otsu, Shiga, Japan) and pE-eco (ecotropic *env*; Takara Bio) with the retroviral vector plasmid pM-LTR-Tat-ZG, pH-LTR-Tat-ZG, or pMT-MFR-PL2. This was performed with use of human embryonic kidney 293T-derived G3T-hi cells (Takara Bio) by using the calcium phosphate co-transfection method. The GALV-*env* retroviral vector was obtained from PG13 packaging cells (ATCC no. CRL-10686) by infection with the ecotropic retrovirus vector as prepared above. After selection of the infected PG13 cells, the virus was collected from the growth medium by filtration of the supernatant with use of a low-protein binding filter (0.45 μm).

Retroviral transduction into CEM-SS cells

CEM-SS cells were infected with self-inactivating retroviral vectors in the presence of 8 μg/ml Polybrene (hexadimethrine bromide; Sigma-Aldrich). Polyclonal gene-transduced cell populations were obtained by selecting the cells with G418 (Invitrogen) at a concentration of 1 mg/ml.

CEM-SS cells or CEM-SS cells transduced with MTD3-U3TAR-MazF were infected with Tat expression retroviral vectors M-LTR-Tat-ZG or H-LTR-Tat-ZG in the presence of RetroNectin (Takara Bio) according to the manufacturer's protocol.

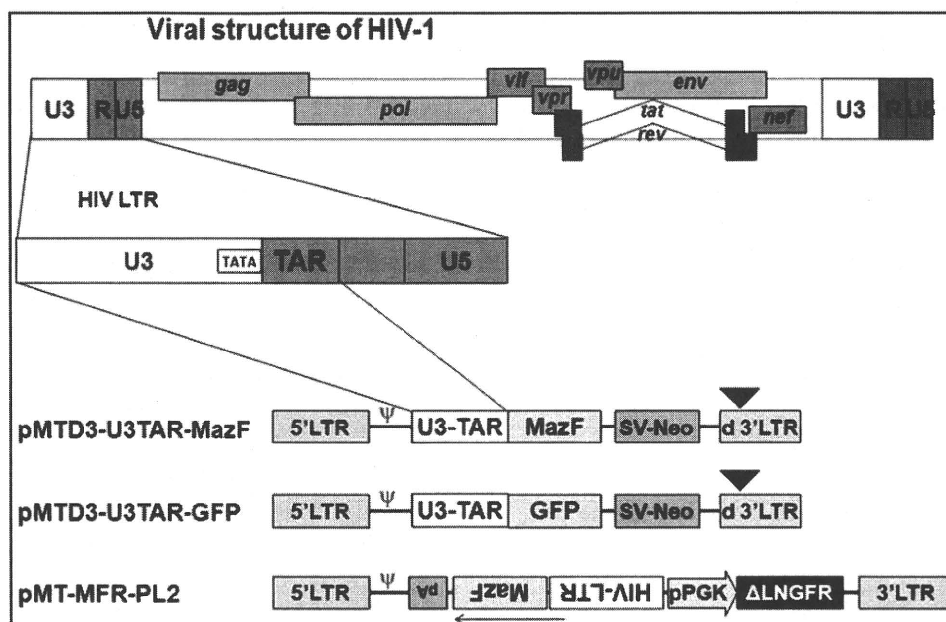

FIG. 1. Construction of retroviral vector under the control of HIV-LTR promoter. To remove promoter activity of the MoMLV LTR, the self-inactivating retroviral vector pMTD3 was constructed based on pMT (Lee *et al.*, 2004) by deleting a 276-bp fragment from its 3′LTR U3 region. A synthetic ACA-less *mazF* gene was then inserted downstream of HIV-1 U3-TAR resulting in the self-inactivating retroviral vector, pMTD3-U3TAR-MazF. As a control, the GFP gene was inserted in place of the *mazF* gene, which resulted in pMTD3-U3TAR-GFP. The self-inactivating retroviral vectors were generated using the transient transfection method with the packaging plasmids MoMLV-gag-pol, GALV-env, and the self-inactivating retroviral vector in 293T cells. The viral preparation was obtained 2 days after transfection by filtering the culture supernatant. To improve the viral titer for efficient gene transduction over an initial vector, HIV-LTR-MazF-polyA cassette was inserted in the opposite direction of the MoMLV-LTR at the multi-cloning site of pMT. A truncated form of the human low-affinity nerve growth factor gene (ΔLNGFR) (Verzeletti *et al.*, 1998) was used as a surface marker. The resultant vector plasmid was designated pMT-MFR-PL2. GALV-env retroviral vector was generated as described in Materials and Methods.

Retroviral transduction into primary rhesus macaque CD4+ T cells

Rhesus macaque CD4+ T cells were isolated from peripheral blood mononuclear cells (PBMC) using anti-CD4 monoclonal antibody-conjugated beads (Dynal CD4 Positive Isolation Kit; Invitrogen). Prior to gene transduction, the isolated CD4+ T cells were activated for 3 days with a combination of anti-monkey-CD3 clone FN-18 (BioSource, Camarillo, CA) and anti-human-CD28 monoclonal antibody clone L293 (BD Biosciences, Franklin Lakes, NJ)-conjugated beads at a cell-to-bead ratio of 1:1 in GT-T503 (Takara Bio) supplemented with 10% FBS and 200 IU of interleukin-2 (Chiron, Emeryville, CA). On day 3, activated CD4+ T cells were infected with the MazF retroviral vector (MT-MFR-PL2) in the presence of RetroNectin (Takara Bio) as per the manufacturer's instructions. The transduction was repeated again on day 4. The cells were further incubated for another 3 days. The genetically modified cells marked with the ΔLNGFR+ were concentrated with anti-CD271 monoclonal antibody-conjugated beads (CD271 MicroBeads; Miltenyi Biotec, Bergisch Gladbach, Germany). Aliquots of the *mazF* gene-modified cells (designated as MazF-Tmac cells) were collected and cryopreserved until use. As a control, the nontransduced CD4+ T cells were also prepared using the same method as used above.

HIV infection

CEM-SS cells and CEM-SS cells transduced with MTD3-U3TAR-MazF or MTD3-U3TAR-GFP were infected with HIV-1 IIIB at the different multiplicities of infection (MOIs) of 0.07, 0.0007, and 0.00007. After infection, cells were washed with PBS and subsequently cultured in 10 ml of RPMI 1640 containing 10% FBS. HIV-1 p24 levels in the culture supernatant were calculated using the p24 ELISA kit (PerkinElmer, Waltham, MA). Viable cell numbers were measured using the trypan blue exclusion assay. The doubling time of cells was calculated by logistic regression analysis of each growth curve for the HIV-1 infection sets.

SHIV infection

The cryopreserved cells of the control CD4+ T and MazF-Tmac cells were recovered in GT-T503 medium supplemented with 10% FBS and 200 IU of interleukin-2 and reactivated with anti-monkey-CD3 and anti-human-CD28 monoclonal antibody-conjugated beads at a cell-to-bead ratio of 5:1. After a 6-day incubation, the cells were infected with simian/human immunodeficiency virus (SHIV) 89.6P (Reimann *et al.*, 1996) at the MOI of 0.01 and cultured for 6 more days. SHIV RNA levels in the culture supernatant and intracellular RNAs were determined by using quantitative real-time PCR (Thermal Cycler Dice Real Time System; Takara Bio Inc.) with a set of specific primers designed in the SHIV *gag* region (Miyake *et al.*, 2006).

Flow cytometry

Flow cytometry was used for the analysis of surface CD4 expression and transduction efficiency. Endogenous expression levels of CD4 in CEM-SS cells and CEM-SS cells transduced with MTD3-U3TAR-MazF were analyzed using phycoerythrin (PE)-labeled anti-human CD4 antibody (Beckman Coulter, Fullerton, CA). Intracellular p24 levels were analyzed using fluorescein isothiocyanate-labeled anti-p24 antibody (Beckman Coulter) after the cells were fixed and permeabilized for flow cytometric analysis.

Gene transfer efficiencies of the retroviral Tat expression vector into CEM-SS cells and CEM-SS cells transduced with MTD3-U3TAR-MazF were analyzed by detecting the ZsGreen marker fluorescence. Immediately before flow cytometry, propidium iodide (PI) was added at the concentration of 100 ng/ml to stain dead cells. Samples were run through a FACSCantoII flow cytometer (BD Biosciences), and data were analyzed using the FACSDiva software (BD Biosciences).

Genomic DNA analysis

Genomic DNA was extracted by phenol/chloroform extraction from CEM-SS cells and CEM-SS cells transduced with MTD3-U3TAR-MazF cells infected with HIV-1 IIIB at the MOI of 0.007. Two different regions of the HIV-1 *gag* gene (246–467 and 905–1046) were amplified by PCR at 14 days after HIV-1 IIIB infection. As a positive control, genomic DNA was amplified from H9 cells chronically infected with HIV-1 IIIB. Human mitochondrial DNA (mtDNA) was amplified as a control for the PCR.

Co-culture with chronically infected cells

The CEM-SS cell line chronically infected with HIV-1 IIIB (CH-1) was mixed with CEM-SS cells or CEM-SS cells transduced with MTD3-U3TAR-MazF. CH-1 cells were mixed at different ratios of 10, 1, or 0.1%. After 6 and 14 days of infection, intracellular p24 levels were analyzed by flow cytometric analyses.

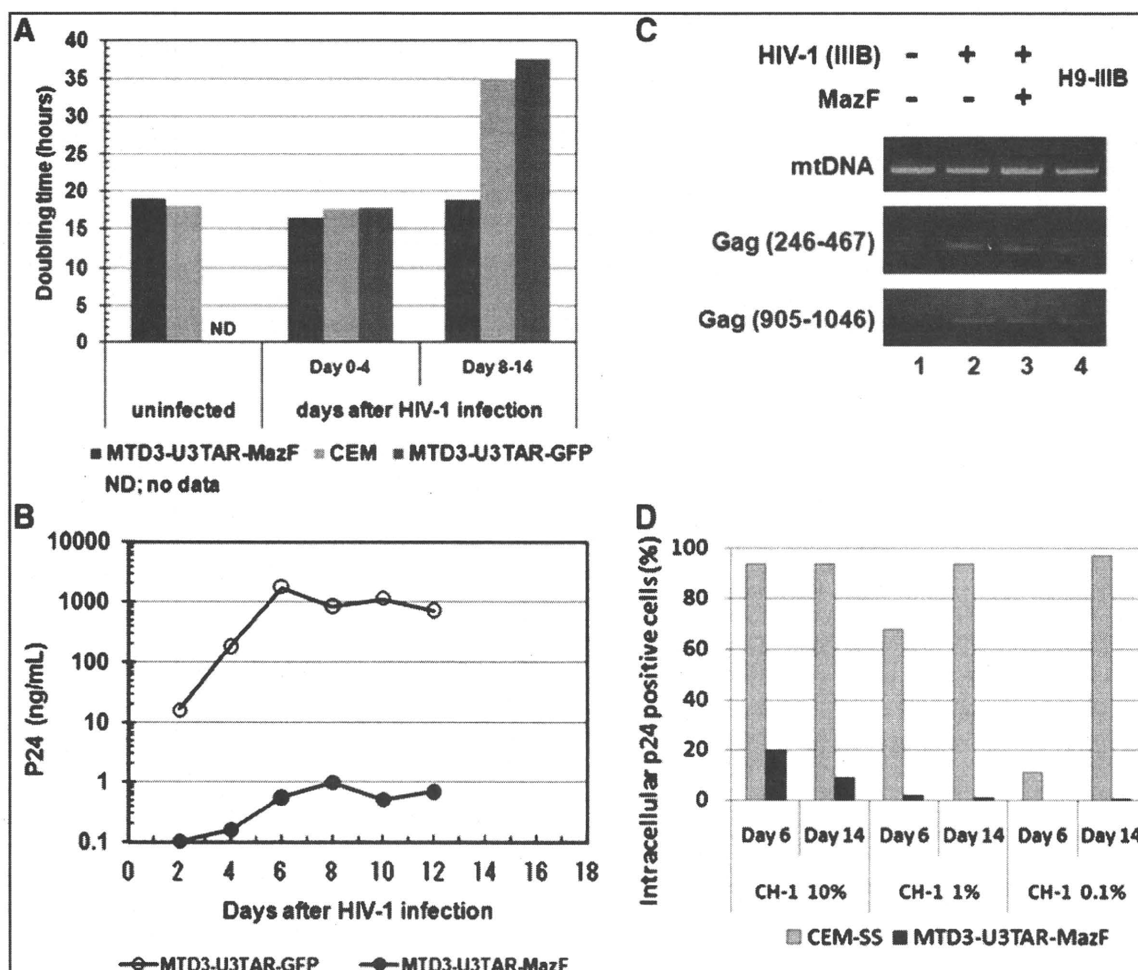

FIG. 2. Analysis of MazF-transduced CEM-SS cells after HIV-1 infection. (**A**) CEM-SS cells transduced with either the *mazF* gene or the GFP gene were infected with HIV-1 IIIB at an MOI of 0.07. After infection, the doubling time of the cells for each culture condition was calculated using linear regression analysis using Microsoft Excel software. The square of the correlation coefficient (R^2) between culture day and log (cell number) values was observed to be >0.97. (**B**) HIV-1 p24 levels in the culture supernatant were estimated using the p24 ELISA kit. Filled circles indicate p24 levels in the supernatant of CEM-SS cells transduced with MTD3-U3TAR-MazF. Open circles indicate p24 levels in the supernatant of CEM-SS cells transduced with MTD3-U3TAR-GFP. (**C**) Genomic DNA PCR analysis of CEM-SS cells and MazF-transduced CEM-SS cells infected with HIV-1 IIIB at an MOI of 0.007. Two different regions of the HIV-1 *gag* gene (246–467 and 905–1046) were amplified by PCR at 14 days after HIV-1 IIIB infection. As a positive control, the genomic DNA was amplified from H9 cells chronically infected with HIV-1 IIIB. Human mtDNA was amplified as a control for the PCR reaction. (**D**) Intracellular p24 levels were analyzed in the mixtures of CEM-SS cell lines chronically infected with HIV-1 IIIB (CH-1) using CEM-SS cells or MazF-transduced CEM-SS cells. CH-1 cells were mixed at different ratios of 10, 1, or 0.1%. After 6 and 14 days of infection, cells were stained with an anti-HIV-1 p24 antibody and subjected to flow cytometric analysis.

Results

We first constructed the retroviral vector system in which the gene for MazF was inserted downstream of the HIV-1 TAR sequence (Fig. 1). As the *E. coli mazF* gene contains nine ACA sequences in its open-reading frame, all of these ACA sequences were first engineered to other MazF-uncleavable sequences without altering the amino acid sequence of MazF to make the *mazF* mRNA resistant to MazF. The resulting self-inactivating retroviral vector (MTD3-U3TAR-MazF) was used to transduce CD4+ T lymphoid CEM-SS cells to create a system in which MazF induction in CEM-SS cells upon infection with HIV-1 effectively suppressed HIV-1 replication without causing apoptosis of infected T cells. The MTD3 retroviral vector contained an intact 5′ LTR and a mutated 3′ LTR that lacks most of the transcriptional elements present in U3. Cells transduced with the resulting retroviral vector contained the defective LTR at both ends (Yu *et al.*, 1986). The self-inactivating retroviral vector was transiently produced and subsequently transduced into the human T lymphoid line CEM-SS cells, which are highly susceptible to HIV infection. Transduced cells were subjected to G418 selection to obtain drug-resistant populations. A GFP-expressing retroviral vector under the control of HIV-LTR (MTD3-U3TAR-GFP) was also used as a control.

The growth rate of CEM-SS cells transduced with MTD3-U3TAR-MazF was comparable to that of the parental CEM-SS line (Fig. 2A), suggesting that MazF expression was tightly controlled and did not inhibit cell growth. Furthermore, the CD4 levels of MTD3-U3TAR-MazF-transduced CEM-SS cells were identical to those of the parental CEM-SS cells (Fig. 3A).

To investigate the effects of HIV-1 infection, MazF-transduced or GFP-transduced CEM-SS cells were infected with HIV-1 IIIB at different MOIs, specifically 0.07, 0.0007, and 0.00007 (Fig. 4). Levels of the HIV-1 p24 antigen in the culture media were examined 16 days post infection. As shown in Fig. 4, in MazF-transduced CEM-SS cells, HIV-1 replication was effectively suppressed. To more precisely investigate the antiviral effects of MazF, viral production and cell growth were measured every other day after HIV-1 IIIB infection at the MOI of 0.07. As shown in Fig. 2A, in the beginning of the culture from day 0 to day 4, cell growth was similar among CEM-SS cells, MazF-transduced CEM-SS cells, and GFP-transduced CEM-SS cells, as well as uninfected CEM-SS cells. CEM-SS cells harboring the *mazF* (ACA-less) gene grew at a normal rate throughout the time course of HIV-1 IIIB infection, whereas both GFP-transduced CEM-SS cells and the parental cell line showed aberrant growth rates due to HIV-1 infection in late cultures after day 8 (Fig. 2A). Indeed, a high level of p24 was detected in the GFP-transduced cell populations during the course of infection (Fig. 2B). In the case of MazF-transduced cells, however, levels of p24 were three orders of magnitude lower than those of GFP-transduced cells throughout the experiment (Fig. 2B). Notably, CD4 levels of MazF-transduced cells infected with HIV-1 IIIB were largely unaffected (Fig. 3B). Together with the fact that the HIV-1 IIIB infected cells harboring the *mazF* gene grew normally (Fig. 2A), these results suggest that HIV-1 IIIB gene expression in the HIV-1-LTR-regulated *mazF* (ACA-less)-transduced cells is effectively inhibited by blocking HIV-1 replication with little damage to cellular function.

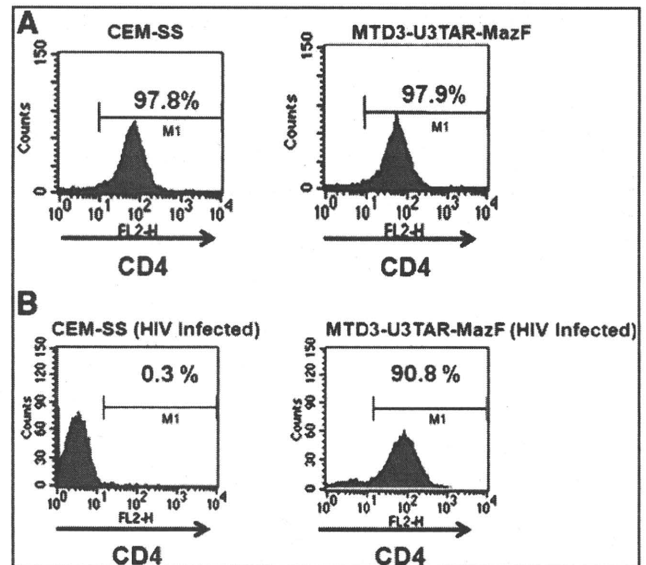

FIG. 3. CD4 levels in MazF-transduced cells. (**A**) Endogenous expression levels of CD4 were analyzed using PE-labeled anti-human CD4 antibody following flow cytometric analysis. (**B**) CEM-SS control cells and CEM-SS cells transduced with MTD3-U3TAR-MazF were infected with HIV-1 IIIB at an MOI of 0.007. After infection, the cells were maintained for 5 weeks and CD4 expression levels were analyzed using PE-labeled anti-human CD4 antibody following flow cytometric analysis.

Next, we examined if HIV-1 IIIB was integrated into the genome of MazF-transduced CEM-SS cells upon HIV-1 infection. Two different regions of the HIV-1 *gag* gene were amplified by PCR using genomic DNA 14 days after HIV-1 IIIB infection. As shown in Fig. 2C, both regions of the *gag* gene were detected in the genome of MazF-transduced CEM-SS cells, which were resistant to HIV-1 replication (lane 3). Similarly, HIV-1 DNA was detected in the genomes of CEM-SS cells (lane 2) and H9-IIIB cells (lane 4) (positive control H9 cells chronically infected with HIV-1 IIIB), whereas no bands were detected in noninfected cells (lane 1). We also established a CEM-SS cell line chronically infected with HIV-1 IIIB (CH-1). When this cell line was mixed with CEM-SS cells or MazF-transduced CEM-SS cells at a ratio of 10, 1, or 0.1%, CEM-SS cells were gradually infected with HIV-1 produced from CH-1 cells (Fig. 2D) and their cell growth was suppressed. Alternatively, MazF-transduced CEM-SS cells showed no growth inhibition (data not shown), indicating that HIV-1 replication was suppressed in MazF-transduced CEM-SS cells. As a result, the culture was eventually taken over by normally growing MazF-transduced CEM-SS cells over the slow-growing CH-1 cells. These data demonstrate that MazF-transduced cells are resistant to HIV-1 IIIB infection by blocking HIV-1 IIIB replication.

To investigate the *mazF* gene expression and subsequent effects more precisely, CEM-SS cells and CEM-SS cells transduced with MTD3-U3TAR-MazF were infected with the Tat-expressing retroviral vectors, M-LTR-Tat-ZG or H-LTR-Tat-ZG (Fig. 5A). Induction of the *mazF* gene in CEM-SS cells transduced with MTD3-U3TAR-MazF was monitored by real-time PCR, and the relative ratios were compared with mock infection (Fig. 5B). Infected cells were also subjected to

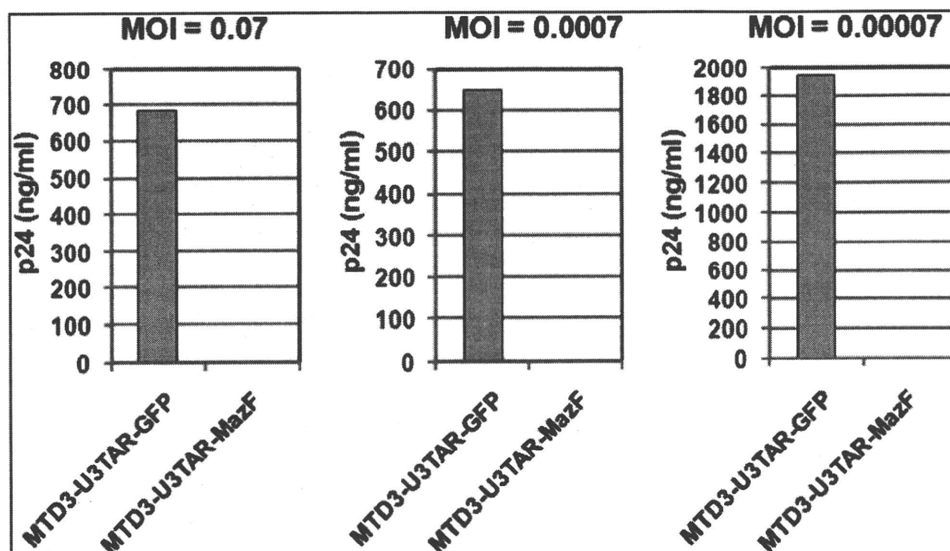

FIG. 4. HIV-1 IIIB infection using MazF-transduced CEM-SS cells at different MOIs. Polyclonal cell populations of CEM-SS resulting from gene transduction with retroviral vectors MTD3-U3TAR-MazF or MTD3-U3TAR-GFP were infected with HIV-1 IIIB at different MOIs (0.07, 0.0007, and 0.00007). Sixteen days after infection, HIV-1 p24 levels in the culture supernatant were estimated using the p24 ELISA kit (PerkinElmer). Given the cytopathic effect of HIV-1, the MTD3-U3TAR-GFP cell population showed delayed proliferation after HIV-1 infection in contrast to the MTD3-U3TAR-MazF population. The delay was more pronounced for the high-MOI group (0.07) than for the low-MOI group (0.00007) at later time points. On day 16 post infection, the accumulated cell number of the high-MOI group was threefold lower than that of the low-MOI group, so the difference in HIV-1 p24 levels between the two MOI groups (0.07 and 0.00007) reflects total cell numbers.

flow cytometry, and both Tat-positive (ZsGreen-positive) cells and dead cells (PI-positive) were monitored (Fig. 5B). As shown in Fig. 5B, strong induction of *mazF* expression was observed upon constitutive M-LTR-Tat-ZG vector transduction, and there was a significant decline in Tat-positive (ZsGreen-positive) cell population. On the other hand, *mazF* induction in HIV-LTR-driven Tat expression was lower, and the influence on cell death was also less than by MLV-LTR-driven Tat expression as observed in the PI-positive population. Although these experiments do not directly reflect HIV-1 replication, these data support the hypothesis that only low levels of MazF are expressed upon HIV-1 infection and MazF-positive cells can survive with HIV-1 provirus.

As the SIN-based retroviral vector contains the *mazF* gene in the normal orientation, the *mazF* gene is expressed from viral mRNA, resulting in the degradation of the viral RNA and thus significantly reducing the viral titer from this vector. On the other hand, when the MazF expression cassette is

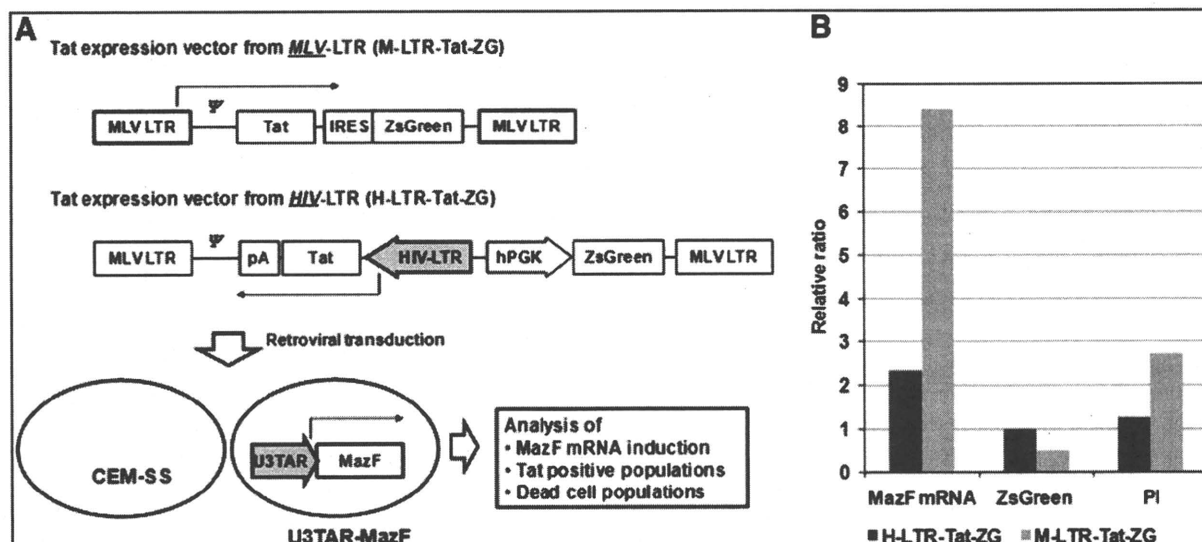

FIG. 5. Analysis of MazF induction upon Tat expression. (A) Outline of experimental procedure to analyze MazF induction upon Tat expression. (B) MazF mRNA levels were analyzed in MTD3-U3TAR-MazF transduced CEM-SS cells after Tat-expressing retroviral vector infection using real-time RT-PCR. The relative fold change is shown compared with that of mock infections. Tat-positive (ZsGreen-positive) cell populations and dead (PI-positive) cell populations in MTD3-U3TAR-MazF-transduced CEM-SS cells were analyzed by flow cytometry 2 days after different Tat retroviral vector transduction. The relative ratio is shown compared with that of CEM-SS cells.

inserted in the opposite direction from the retroviral genome, the viral titer increased and the gene transfer efficiency was improved more than 10 times (data not shown). To investigate the antiviral effect of the TAR-*mazF* system in the primary CD4+ T lymphocytes, the reversely orienting MT-MFR-PL2 vector was introduced into rhesus macaque primary CD4+ T cells from two individual monkeys (#14 and #15). The resulting *mazF*-containing cells were then infected with SIV/HIV-1 chimeric virus SHIV 89.6P. As the SHIV 89.6P harbors HIV-1-derived *env*, *rev*, *vpu*, and *tat* genes, the TAR-*mazF* system is expected to function when MazF-Tmac cells are infected with SHIV 89.6P. Indeed, efficient suppression of SHIV 89.6P replication was observed for both primary cell lines, #14 and #15 (Fig. 6A).

To evaluate further how well the retroviral *mazF* system is able to suppress viral RNA production, total cellular RNAs were extracted from MazF-Tmac cells to estimate quantitatively the amounts of SHIV RNA, as well as the mRNAs for ribosomal protein L13a (RPL13a, XM_001093017) and β-actin (NM_001033084), by real-time PCR. The relative ratios were normalized by using 18S rRNA (FJ436026), which is protected from MazF cleavage in ribosomes (Shimazu *et al.*, 2007). We obtained similar results in MazF-Tmac cells from both #14 and #15 primary cell lines. Representative results from MazF-Tmac cells from #14 are shown in Fig. 6B, where one can see that SHIV RNA was preferentially cleaved, whereas the cellular mRNAs were not affected. These results clearly demonstrate that MazF induction from the Tat system upon SHIV 89.6P infection leads to severe defect in maintaining SHIV 89.6P RNA but does not affect cellular mRNAs in SHIV-infected CD4+ T cells.

Discussion

This study demonstrates the distinct feasibility of RNase-based strategies for gene therapy. RNase-based strategies may be preferred over RNA-based strategies for HIV therapy, because RNases cleave HIV-RNA to cause permanent damage to HIV RNA function. Additionally, as RNases function as an enzymatic catalyst, they are required only at low concentrations in the cells to effectively block HIV proliferation. In the present study, the gene for MazF, an ACA-specific mRNA interferase, was engineered under the HIV-1 LTR promoter and inserted in the genome of the CD4+ T lymphoid cells so that MazF is expected to be produced only when the cells are infected with HIV-1 to produce the Tat protein. We demonstrated that *mazF*-Tmac cells indeed acquired resistance against SHIV replication, but cell growth was not inhibited after SHIV infection (data not shown), indicating that cellular mRNAs were not significantly affected. Notably, MazF was also able to function against the expression of SHIV proviral genome, because the production of SHIV in the culture supernatant was dramatically reduced.

Acquisition of HIV-1 resistance, and more remarkably the ability of MazF-transduced cells to suppress HIV-1 replication, may be explained as follows: Upon HIV-1 infection, Tat expression is first induced from the HIV-1 proviral genome. Tat then triggers the transcription of the *mazF* gene under the LTR promoter, as well as the full-length HIV proviral genome. The resulting induction of MazF expression leads to the cleavage of newly emerged HIV-1 mRNAs so that Tat protein synthesis is no longer sustainable. However, it is important to note that HIV-1 infection does not hamper cell growth and that the HIV-1 provirus genome is retained in the MazF-transduced cells. Therefore, the cellular level of Tat appears to be maintained at a very low level so that the level of MazF induction is also kept very low enough to cleave HIV-1 mRNAs, but not cellular mRNAs. Depending on the integration site and proviral copy number, there might be some MazF-transduced cells that were not resistant to HIV-1 replication. However, these cells could not survive due to HIV-1-induced cell death.

In mammals, virus infection is known to activate the interferon response to induce RNaseL, which mediates degradation of 28S and 18S ribosomal RNAs. This results in inhibition of protein synthesis as part of the host antiviral response (Silverman, 2003). An amphibian ribonuclease,

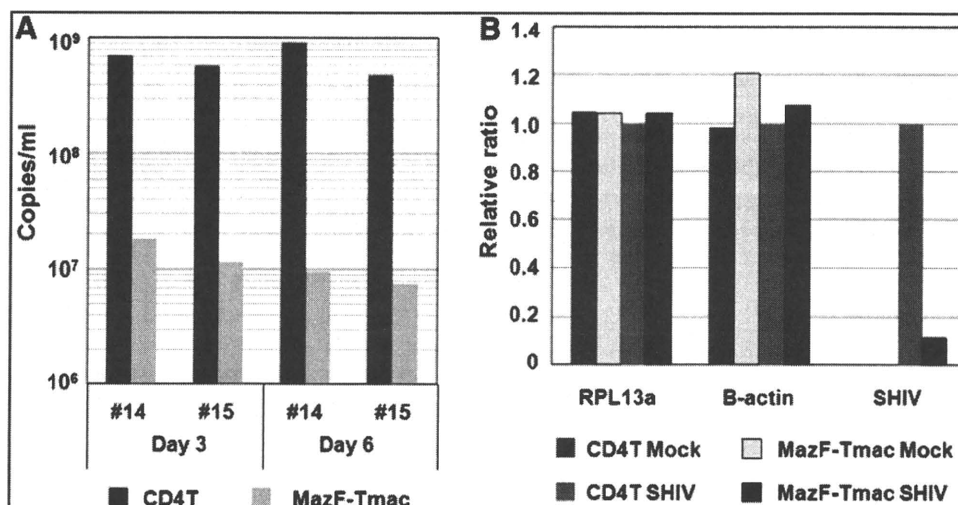

FIG. 6. Effect of MazF-induction into rhesus macaque primary CD4+ T cells on SHIV 89.6P replication. **(A)** Rhesus macaque primary CD4 T cells from two monkeys (#14 and #15) were activated and transduced with MT-MFR-PL2 vector. The MazF-transduced cells (MazF-Tmac cells) were reactivated with CD3/28 beads followed by infection with SHIV 89.6P. On days 3 and 6 post infection, culture supernatants were collected and evaluated for SHIV RNA copy by using the quantitative real-time PCR method. **(B)** Total cellular RNAs extracted from MazF-Tmac cells at 6 days post SHIV 89.6P infection were used to measure the amounts of SHIV RNA, as well as cellular housekeeping mRNAs, by using the quantitative real-time PCR method.

Onconase, is able to inhibit protein synthesis in mammalian cells and has been used as a protein drug. When it was added to the culture media of H9 cells persistently infected with HIV-1, HIV-1 replication was inhibited without blocking cell growth, as degradations of 18S and 28S rRNAs and cellular mRNAs were prevented (Saxena *et al.*, 1996). MazF induction in mammalian cells has shown to cause apoptotic cell death as a result of degradation of cellular mRNAs (Shimazu *et al.*, 2007). However, in the present study, MazF expression induced by HIV-1 Tat appears to be maintained at very low levels, just enough to cleave HIV-1 RNA but not cellular mRNAs, so that cells were able to grow normally. MazF expression may be autoregulated in the cell in such a way that when Tat-induced MazF eliminates invading HIV-1 RNA, Tat expression from the HIV-1 provirus is simultaneously stopped, resulting in simultaneous arrest of MazF production to recover normal cellular functions.

Targeting HIV RNA as a therapeutic strategy using antisense RNA (Levine *et al.*, 2006), ribonucleases (Agarwal *et al.*, 2006), and RNA interference (RNAi) technology (Morris and Rossi, 2004) has been attempted. However, the use of antisense RNA and RNAi technology has not been effective as an anti-HIV technology, as HIV can easily circumvent these RNA inhibitors by creating mutations at the target sequence regions (Lee and Rossi, 2004). On the other hand, the present strategy using MazF targets abundant ACA sequences in HIV-1 RNA (>240), so that it is not possible for HIV-1 to escape from MazF attack by mutations. Furthermore, because MazF has no homology to any mammalian ribonucleases, MazF mRNA interferase activity cannot be inhibited by ribonuclease inhibitors existing in mammalian cells.

In summary, the use of MazF appears to be a novel and highly effective tool for anti-HIV gene therapy. It is effectively able to suppress HIV-1 replication, preventing the emergence of mutated HIV-1. Importantly, MazF induction by invading HIV-1 shows little toxicity to host cells while it efficiently suppresses HIV-1 replication. Specific inhibition of HIV-1 replication by MazF without affecting cell growth is the key feature of MazF-based HIV-1 gene therapy. This may be the first step for RNase-based HIV-1 gene therapy with efficacy *in vitro*. The feasibility of the MazF-based *ex vivo* gene therapy may be verified using autologous CD4+ T lymphocytes from HIV-1 patients. To use our *mazF* vector system for gene therapy, its safety has to be critically evaluated and it should not have any negative impacts on T-cell function. For example, it needs to be shown that there is no alteration in the secretion of functionally important cytokines even though it was observed that MazF expression in HIV-infected CD4+ T cells does not inhibit cell growth. We are currently addressing this question.

Acknowledgments

The authors thank Dr. Keith A. Reimann of Harvard Medical School and Dr. Tomoyuki Miura of Kyoto University for providing the SHIV 89.6P. The authors also thank Dr. Koich Inoue of Takara Bio Inc. for his critical reading of the manuscript.

Author Disclosure Statement

No competing financial interests exist.

References

Agarwal, S., Nikolai, B., Yamaguchi, T., Lech, P., and Somia N.V. (2006). Construction and use of retroviral vectors encoding the toxic gene barnase. Mol. Ther. 14, 555–563.

Berkhout, B., Silverman, R.H., and Jeang, K.T. (1989). Tat trans-activates the human immunodeficiency virus through a nascent RNA target. Cell 59, 273–282.

Kim, S., Ikeuchi, K., Byrn, R., Groopman, J., and Baltimore, D. (1989). Lack of a negative influence on viral growth by the nef gene of human immunodeficiency virus type 1. Proc. Natl. Acad. Sci. U.S.A. 86, 9544–9548.

Lee, J.T., Yu, S.S., Han, E., Kim, S., and Kim, S. (2004). Engineering the splice acceptor for improved gene expression and viral titer in an MLV-based retroviral vector. Gene Ther. 11, 94–99.

Lee, N.S., and Rossi, J.J. (2004). Control of HIV-1 replication by RNA interference. Virus Res. 102, 53–58.

Levine, B.L., Humeau, L.M., Boyer, J., MacGregor, R.R., Rebello, T., Lu, X., Binder, G.K., Slepushkin, V., Lemiale, F., Mascola, J.R., Bushman, F.D., Dropulic, B., and June, C.H. (2006). Gene transfer in humans using a conditionally replicating lentiviral vector. Proc. Natl. Acad. Sci, U.S.A. 103, 17372–17377.

Miyake, A., Ibuki, K., Enose, Y., Suzuki, H., Horiuchi, R., Motohara, M., Saito, N., Nakasone, T., Honda, M., Watanabe, T., Miura, T., and Hayami, M. (2006). Rapid dissemination of a pathogenic simian/human immunodeficiency virus to systemic organs and active replication in lymphoid tissues following intrarectal infection. J. Gen. Virol. 87, 1311–1320.

Morris, K.V., and Rossi, J.J. (2006). Lentivirus-mediated RNA interference therapy for human immunodeficiency virus type 1 infection. Hum. Gene Ther. 17, 479–486.

Nariya, H., and Inouye, M. (2008). MazF, an mRNA interferase, mediates programmed cell death during multicellular Myxococcus development. Cell 132, 55–66.

Reimann, K.A., Li, J.T., Voss, G., Lekutis, C., Tenner-Racz, K., Racz, P., Lin, W., Montefiori, D.C., Lee-Parritz, D.E., Lu, Y., Collman, R.G., Sodroski, J., and Letvin, N.L. (1996). An env gene derived from a primary human immunodeficiency virus type 1 isolate confers high in vivo replicative capacity to a chimeric simian/human immunodeficiency virus in rhesus monkeys. J. Virol. 70, 3198–3206.

Saxena, S.K., Gravell, M., Wu, Y.N., Mikulski, S.M., Shogen, K., Ardelt, W., and Youle, R.J. (1996). Inhibition of HIV-1 production and selective degradation of viral RNA by an amphibian ribonuclease. J. Biol. Chem. 271, 20783–20788.

Shimazu, T., Degenhardt, K., Nur-E-Kamal, A., Zhang, J., Yoshida, T., Zhang, Y., Mathew, R., White, E., and Inouye, M. (2007). NBK/BIK antagonizes MCL-1 and BCL-XL and activates BAK-mediated apoptosis in response to protein synthesis inhibition. Genes Dev. 21, 929–941.

Silverman, R.H. (2003). Implications for RNase L in prostate cancer biology. Biochemistry 42, 1805–1812.

Verzeletti, S., Bonini, C., Marktel, S., Nobili, N., Ciceri, F., Traversari, C., and Bordignon, C. (1998). Herpes simplex virus thymidine kinase gene transfer for controlled graft-versus-host disease and graft-versus-leukemia: clinical follow-up and improved new vectors. Hum. Gene Ther. 9, 2243–2251.

Yamaguchi, Y., and Inouye, M. (2009). mRNA interferases, sequence-specific endoribonucleases from the toxin-antitoxin systems. Prog. Mol. Biol. Transl. Sci. 85, 467–500.

Yu, S.F., von Rüden, T., Kantoff, P.W., Garber, C., Seiberg, M., Rüther, U., Anderson, W.F., Wagner, E.F., and Gilboa, E.

(1986). Self-inactivating retroviral vectors designed for transfer of whole genes into mammalian cells. Proc. Natl. Acad. Sci. U.S.A. 83, 3194–3198.

Yu, S.S., Han, E., Hong, Y., Lee, J.T., Kim, S., and Kim, S. (2003). Construction of a retroviral vector production system with the minimum possibility of a homologous recombination. Gene Ther. 10, 706–711.

Zhang, Y., Zhang, J., Hoeflich, K.P., Ikura, M., Qing, G., and Inouye, M. (2003). MazF cleaves cellular mRNAs specifically at ACA to block protein synthesis in *Escherichia coli*. Mol. Cell 12, 913–923.

Zhu, L., Zhang, Y., The, J.S., Zhang, J., Connell, N., Rubin, H., and Inouye, M. (2006). Characterization of mRNA interferases from Mycobacterium tuberculosis. J. Biol. Chem. 281, 18638–18643.

Zhu, L., Inoue, K., Yoshizumi, S., Kobayashi, H., Zhang, Y., Ouyang, M., Kato, F., Sugai, M., and Inouye, M. (2009). *Staphylococcus aureus* MazF specifically cleaves a pentad sequence, UACAU, which is unusually abundant in the mRNA for pathogenic adhesive factor SraP. J. Bacteriol. 191, 3248–3255.

Address correspondence to:
Dr. Ikunoshin Kato
Center for Cell and Gene Therapy
Takara Bio Inc.
Seta 3-4-1
Otsu, Shiga
520-2193, Japan

E-mail: ikukatiku@zeus.eonet.ne.jp

Dr. Masayori Inouye
Department of Biochemistry
Robert Wood Johnson Medical School
675 Hoes Lane
Piscataway, NJ 08854, USA

E-mail: inouye@umdnj.edu

Received for publication January 5, 2010; accepted after revision July 22, 2010.

Published online: July 22, 2010.

Author's personal copy

Vaccine 28S (2010) B75–B77

ELSEVIER

Contents lists available at ScienceDirect

Vaccine

journal homepage: www.elsevier.com/locate/vaccine

Review

Establishment of specific pathogen-free macaque colonies in Tsukuba Primate Research Center of Japan for AIDS research

Yasuhiro Yasutomi [a,b,*]

[a] *Laboratory of Immunoregulation and Vaccine Research, Tsukuba Primate Research Center, National Institute of Biomedical Innovation, Tsukuba, Ibaraki 305-0843, Japan*
[b] *Department of Immunoregulation, Mie University Graduate School of Medicine, Mie 514-8507, Japan*

ARTICLE INFO

Article history:
Received 9 April 2009
Received in revised form 13 August 2009
Accepted 18 September 2009

Keywords:
Macaque
SPF
Virus

ABSTRACT

Cynomolgus monkeys have been maintained in indoor facilities as closed colony monkeys in Tsukuba Primate Research Center in Japan since 1978. Several microorganisms, including bacteria, parasites and viruses, were eliminated from the cynomolgus monkeys in this colony of TPRC. Various kinds of viruses (B virus, measles virus, simian varicella virus, simian immunodeficiency virus, simian T cell leukemia virus, simian D type retrovirus, simian cytomegalovirus, simian Epstein-Barr virus, and simian foamy virus), bacteria (*Shigella*, *Salmonella* and *Mycobacteria spp.*) and intestinal helminth were chosen as target microorganisms to establish a specific pathogen-free (SPF) colony. Except for a few pathogens (simian D type retrovirus, simian Epstein-Barr virus, and simian foamy virus), selected pathogens were completely eliminated from all monkeys in TPRC. In this review, the history of establishment of SPF cynomolgus monkey colonies in Japan is described.

© 2009 Elsevier Ltd. All rights reserved.

Contents

1. Introduction B75
   1.1. First term (1978–1882) B76
   1.2. Second and third terms (1983–1994) B76
   1.3. Fourth and fifth terms to present (1995–2009) B77
2. Conclusions B77
   Acknowledgements B77
   Conflict of interest statement B77
   References B77

1. Introduction

Nonhuman primates are critical resources for biomedical research. Macaque monkeys are one of the key nonhuman primate models that share nearly all characteristics with humans. Conditions of experimental animals are very important for biomedical experiments. The animals should not be infected with microorganisms because microorganism infection may affect results. Moreover, some pathogens are likely to harm not only monkeys but also humans in experiments involving macaques. For these reasons, there is a need for specific pathogen-free (SPF) macaque colonies for research purposes, biohazard avoidance and maintenance of health levels in established colonies (Table 1).

Tsukuba Primate Research Center (TPRC) in Japan has a large-scale breeding colony of experimental cynomolgus monkeys (approximately 1500 monkeys), which play a significant role in the development of pharmaceutical products and medical technologies. The center is the forefront facility in Japan that both supplies laboratory-bred monkeys, mainly cynomolgus monkeys, and performs medical research. Cynomolgus monkeys have been maintained in indoor facilities as closed colony monkeys in TPRC since 1978 [1]. In addition to quality control, supply, research resource development, and basic technology development involving the experimental monkeys, evaluation of state-of-the-art medical technology, evaluation of the efficacy of new drugs and safety assessments are also performed using the monkeys. The establishment of SPF macaques is therefore necessary in TPRC.

* Laboratory of Immunoregulation and Vaccine Research, Tsukuba Primate Research Center, National Institute of Biomedical Innovation, 1-1 Hachimandai, Tsukuba, Ibaraki 305-0843, Japan. Tel.: +81 29 837 2073; fax: +81 29 837 2053.
E-mail addresses: yasutomi@nibio.go.jp, yasutomi@doc.medic.mie-u.ac.jp.

0264-410X/$ – see front matter © 2009 Elsevier Ltd. All rights reserved.
doi:10.1016/j.vaccine.2009.09.079

Author's personal copy

Table 1
History of establishment of SPF cynomolgus monkeys in TPTC.

Year	Target microorganism	Complete elimination from TPRC
1978–1982	BV, MV, *Shigella*, *Salmonella*, *Mycobacteria*, helminth	MV, *Shigella*, *Salmonella*, *Mycobacteria*,
1983–1994	BV, SVV, SIV, STLV-1, SRV/D helminth	SIV, STLV-1, helminth
1995–2004	BV, SVV, SRV/D,	BV, SVV,
2004–Present	SRV/D (73%)[a], LCV (50%)[a], SFV (31%)[a]	CMV

[a] Infection rate of all cynomolgus monkeys in TPRC at present.

The cynomolgus monkeys in TPRC were obtained from Indonesia, Malaysia and Philippines [1]. The monkeys have been bred as pure blood of each origin without interbreed crossing. These pure blood monkeys should be important for comparison of various genetic effects in biological studies including vaccine development. The establishment of SPF colonies in TPRC is also important for this reason. These three pure blood colonies and one mixed blood colony each consist of approximately 100 SPF cynomolgus monkeys. In this review, attempts to establish SPF macaque colonies for advanced biomedical research are reported.

1.1. First term (1978–1882)

Several kinds of microorganisms were chosen for elimination from colony monkeys. Two viruses (B virus and measles virus), three species of bacteria (*Shigella*, *Salmonella* and *Mycobacteria spp.*) and intestinal helminths were selected as the first target pathogens for elimination in macaque colonies. B virus (BV, *Cercopithecine herpesvirus* 1) is an alphaherpesvirus that naturally infects macaque monkeys. In macaques, the virus typically causes a self-limiting disease similar to herepes simplex virus disease in humans [2]. In surprising contrast, BV infection in humans has resulted in the death of 80% of individuals [2]. Therefore, BV was firstly chosen as an SPF target pathogen for prevention of biohazard risks by this virus. The BV infections were detected by BV-specific antibody (Ab) response in sera using an ELISA system (BioReliance Co., USA). Prevention of the spread of BV in the macaque colony was carried out by early weaning of babies from mothers. Infection of the virus in plasma of the prematurely weaned monkeys was confirmed by a BV-specific Ab several times at intervals of 3–6 months. Measles, caused by measles virus (MV) infection, remains a major cause of infant mortality despite the availability of a safe and effective live attenuated virus vaccine. MV-free cynomolgus monkeys are required, since one of the purposes to supply cynomolgus monkeys in TPRC is certification tests for human measles vaccine. MV infection was examined in all monkeys by detection of specific Ab reaction in sera by ELISA and MV antigen (Ag) detected by RT-PCR. Although most of the cynomolgus monkeys from Asia were infected with MV, asymptomatic monkeys with MV excretion in plasma, urine and other biological fluid were not reproduced in TPRC. The MV-infected monkeys were eliminated by this breeding program. Two species of bacteria, *Salmonella* and *Shigella spp.*, were detected by cultivation of rectal or fecal swab samples. Monkeys having these bacteria received drug treatment (200 mg of sulfamethoxazole and 40 mg of trimethoprim once a day for 3 days by oral administration even to *Salmonella*, 200 mg of fosofomycin once a day for 3 days by oral administration even to *Shigella*) if they showed no clinical symptoms of infection with these bacteria. Infection with *Mycobacteria spp.* responsible for tuberculosis was examined by tuberculin (TB) skin tests, and monkeys with positive results of TB skin tests were eliminated. Infection with MV, *Salmonella*, *Shigella* or *Mycobacteria spp.* has not been detected in any monkeys in TPRC since 1982. Cynomolgus monkeys excreting helminth eggs in feces were given anthelimintics (ivermectin 200 μg/kg s.c twice for 2 weeks interval; metronidazol 40 mg/kg once a day for 5 days by oral administration; thiabendazole 50 mg/kg once a day for 3 days by oral administration and mebendazole 20 mg/kg once a day for 3 days by oral administration).

1.2. Second and third terms (1983–1994)

In addition to targeting BV and helminths for elimination from TPRC, simian immunodeficiency virus (SIV), simian T cell leukemia virus (STLV), simian D type retrovirus (SRV/D) and simian varicella virus (SVV) were newly targeted to establish SPF monkey colonies in 1983–1994. Although an AIDS model induced by SIV is very useful for AIDS studies, SIV is not present in macaques from Asia unless they have been experimentally exposed. In fact, natural infection with SIV was not seen in any of the monkeys in TPRC examined by ELISA for detection of SIV-specific Ab in sera. STLV is widely present in all New and Old World primate species. The incidence of STLV infection in most natural simian populations is 5–40%, but it can be much higher in wild monkeys [3,4]. STLV infection was detected in 11.7% of the monkeys in TPRC by IFA using MT-1 cells [5]. These monkeys were eliminated from TPRC over a period of several years. SVV is an alphaherpesvirus that causes varicella in Old World monkeys and establishes latent infection in ganglionic neurons [6]. Outbreaks in many animal facilities have been reported [7]. An outbreak of SVV infection occurred in TPRC during the period from November 1989 to April 1990. Varicella developed in almost 100 monkeys, and 67% of those monkeys died. The rate of infection with SVV in TPRC was 12.9% in 1990. SVV infection can usually be detected by SVV-specific Abs, even in asymptomatic monkeys, and SVV-infected monkeys were eliminated from TPRC in 2000. Attention must be paid to SRV/D both for its risk to macaque colony health and its negative effects on biomedical research. Monkeys infected with SRV/D eventually show symptoms that might be caused by SRV/D infection, such as diarrhea, weight loss and anemia, due to activation attributable to changing conditions of the individual [8–11]. This virus can be transmitted horizontally, vertically or sexually by symptomatic or asymptomatic animals. Moreover, some SRV/D-infected monkeys can become viremic yet remain Ab-negative, allowing infection to escape detection by routine Ab screening [12]. A new subtype of SRV/D, named SRV/D-T, was detected in the colony in TPRC in 2005 [13]. Certain monkeys were found to have plasma viremia of this subtype and did not develop any specific Abs to SRV/D-T. Cynomolgus monkeys in the colony showing SRV/D-T viremia secreted the virus in saliva, urine and feces, and the viruses secreted from these monkeys were thought to be a potential cause of horizontal infections of SRV/D-T. Moreover, there was a high rate of transmission of SRV/D-T infection between mothers and infants in TPRC. Screening for this virus infection was done by detection of both Ab (Western blot analysis) and virus (RT-PCR) in plasma [14]. STLV was completely eliminated from TPRC during the second and third terms.

Author's personal copy

1.3. *Fourth and fifth terms to present (1995–2009)*

Monkey infected with BV and SVV were completely eliminated from TPRC in the late 90s. Three viruses, simian cytomegalovirus (CMV), simian Epstein-Barr virus (EBV, simian lymphocryptoviruses (LCV)) and simian foamy virus (SFV), were added as target viruses in a new plan in 1995 to establish SPF monkey colonies. Simian CMV infections have been reported in various species of monkeys, including macaques [15]. This virus is readily transmitted in oral secretions, breast milk and urine [16], and 3% of adult monkeys in TPRC were infected with the virus. CMV infection was detected by IFA or an ELISA system using CMV Ag. Simian EBV has also been detected in several species of Old World and New World primates [17]. This virus is also readily transmitted, and serological surveys indicated that about 90% of adult cynomolgus monkeys in TPRC were infected. Detection of EBV infection was usually done by using commercial available human IFA kit. Infection with these two viruses, CMV and EBV, in macaques are opportunistic infections. Infection with the other virus, SFV, also does not seem to cause disease in nonhuman primates as natural hosts [18]. Humans can be infected with SFV, although the number of known SFV infection cases in humans is small [19]. SFV infection was detected by IFA using SFV Ag. Monkeys infected with SFV are fraught with hazards to workers in a primate center. The rate of infection with SFV in adult monkeys in TPRC was 80%. Detection of SFV was done by Ab response in sera using ELISA. Prevention of the spread of these three viruses, CMV, LCV and SFV, was performed by artificial nursing with feeding formula for baby monkeys that had been removed from their mothers immediately after birth. CMV infection in monkeys has not been detected in TPRC since 2005.

2. Conclusions

SPF nonhuman primate colonies are required for biomedical research with several beneficial effects such as animal health and occupational safety. High quality of laboratory animals is also required for advanced biomedical studies including vaccine research and development. Infectious agents frequently affect the results of animal experiments. The history of establishment of SPF cynomolgus monkeys in TPRC in Japan for evaluation of state-of-the-art medical technology, evaluation of the efficacy of new drugs and new vaccines, and safety assessments has been described in this review.

Acknowledgements

The author would like to thank all workers in TPRC since 1978 for establishing SPF macaque colonies in Japan.

This study was supported by grants from the Ministry of Health, Labor and Welfare of Japan and the Ministry of Education, Culture, Sports, Science and Technology of Japan.

Conflict of interest statement

The author states that they have no conflict of interest.

References

[1] Honjo S. The Japanese Tsukuba Primate Center for Medical Science (TPC): an outline. J Med Primatol 1985;14:75–89.

[2] Whilley RJ, Hillard J. Cercopithecine herpes virus (B virus). In: Knipe DM, Howley PM, Griffin DE, Lamb RA, Martin MA, Roizman B, et al., editors. Fields virology, vol. 2, 5th ed. Philadelphia, PA: Lippincott Williams & Wilkins; 2007. p. 2889–903.

[3] Richards AL, Girl A, Iskandriatl D, Pamgukas J, Sle A, Rosen L, et al. Simian T lymphotropic virus type I infection among wild-caught Indonesian pig-tailed macaques (*Macaque nemastrina*). J AIDS Hum Retrovirol 1998;19: 542–5.

[4] Schillaci M, Jones-Engel L, Engel G, Paramastri Y, Iskandar E, Willson B, et al. Prevalence of enzootic simian viruses among urban performance monkeys in Indonesia. Trop Med Int Health 2005;10:1305–14.

[5] Hayami M, Komuro A, Nozawa K, Shotake T, Ishikawa K, Yamamoto K, et al. Prevalence of antibody to adult T-cell leukemia virus-associated antigens (ATLA) in Japanese monkeys and other non-human primates. Int J Cancer 1984;33:179–83.

[6] Gray WL, Mullis L, Soike KF. Viral gene expression during acute simian varicella virus infection. J Virol 2002;83:841–6.

[7] Gray WL. Simian varicella: a model for human varicella-zoster virus infections. Rev Med Virol 2004;14:363–81.

[8] Daniel MD, Norval KW, Letvin NL, Hunt RD, Sehgal PK, Desrosiers RC. A new type D retrovirus isolated from macaques with an immunodeficiency syndrome. Science 1984;223:602–5.

[9] Marx PA, Maul DH, Osborn KG, Lerche NW, Moody P, Lowenstine LJ, et al. Simian AIDS: isolation of a type D retrovirus and transmission of the diseases. Science 1984;223:1083–6.

[10] Lerche NW, Osborn KG. Simian retrovirus infections: potential confounding variables in primate toxicology studies. Toxicol Pathol 2003;31(Suppl.):103–10.

[11] Guzman RE, Kerlin RL, Zimmerman TE. Histologic lesions in cynomolgus monkeys (*Macaca fascicularis*) naturally infected with simian retrovirus type D: comparison of seropositive, virus-positive, and uninfected animals. Toxicol Pathol 1999;27:672–7.

[12] Kwng HS, Pederson NC, Lerche NW, Osborn KG, Marx PA, Gardner MB. Viremia, antigenemia and serum antibodies in rhesus macaques infected with simian retrovirus type I1 and their relationship to disease course. Lab Invest 1987;56:591–7.

[13] Hara M, Sata T, Kikuchi T, Nakajima N, Uda A, Fujimoto K, et al. Isolation and characterization of new simian retrovirus type D subtype from monkeys at the Tsukuba Primate Center, Japan. Microbes Infect 2005;7:126–31.

[14] Hara M, Kikuchi T, Ono F, Takano J, Ageyama N, Fujimoto K, et al. Survey of captive cynomolgus macaques colonies for SRV/D infection using polymerase chain reaction assays. Comp Med 2005;55:145–9.

[15] Elkington R, Shouskry NH, Walker S, Crough T, Fazou C, Kaur A, et al. Cross-reactive recognition of human and primate cytomegalovirus sequences by human CD4 cytotoxic T lymphocytes for glycoprotein B and H. Eur J Immunol 2004;34:3216–26.

[16] Barry PA, Loxkridge KM, Salamat S, Tinling SP, Yue Y, Zhou SS, et al. Non-human primate models of intrauterine cytomegalovirus infection. ILAR J 2006;47:49–64.

[17] Cho Y-G, Ramer J, Rivaller P, Quink C, Garber RL, Beler DR, et al. An Epstein-Barr-related herpesvirus from marmoset lymphomas. Proc Natl Acad Sci USA 2001;98:1224–9.

[18] Linial ML. Foamy viruses. In: Knipe DM, Howley PM, Griffin DE, Lamb RA, Martin MA, Roizman B, et al., editors. Fields virology. 5th ed. Philadelphia, PA: Lippincott Williams & Wilkins; 2007. p. 2245–63.

[19] Jones-Engel L, May CC, Engel GA, Steinkraus KA, Schillaci MA, Fuentes A, et al. Diverse contexts of zoonotic transmission of simian foamy viruses in Asia. Emerg Infect Dis 2008;14:1200–8.

Comparative Medicine
Copyright 2010
by the American Association for Laboratory Animal Science

Vol 60, No 1
February 2010
Pages 51–53

Simian Betaretrovirus Infection in a Colony of Cynomolgus Monkeys (*Macaca fascicularis*)

Koji Fujiomto,[1,2,*] Jun-ichiro Takano,[1,2] Toyoko Narita,[1] Koji Hanari,[1] Nobuhiro Shimozawa,[2] Tadashi Sankai,[2] Takashi Yosida,[2] Keiji Terao,[2] Takeshi Kurata,[1] and Yasuhiro Yasutomi[2]

Of the 419 laboratory-bred cynomolgus macaques (*Macaca fascicularis*) in a breeding colony at our institution, 397 (95%) exhibited antibodies or viral RNA (or both) specific for simian betaretrovirus (SRV) in plasma. Pregnant monkeys (*n* = 95) and their offspring were tested to evaluate maternal–infant infection with SRV. At parturition, the first group of pregnant monkeys (*n* = 76) was antibody-positive but RNA-negative, the second group (*n* = 14 monkeys) was positive for both antibody and RNA, and the last group (*n* = 5) was antibody-negative but RNA-positive. None of the offspring delivered from the 76 antibody-positive/RNA-negative mothers exhibited viremia at birth. Eight of the offspring (including two newborns delivered by caesarian section) from the 14 dually positive mothers exhibited SRV viremia, whereas the remaining 6 newborns from this group were not viremic. All of the offspring (including 2 newborns delivered by caesarian section) of the 5 antibody-negative/RNA-positive mothers exhibited viremia at birth. One neonatal monkey delivered by CS and two naturally delivered monkeys that were viremic at birth remained viremic at 1 to 6 mo of age and lacked SRV antibodies at weaning. Family analysis of 2 viremic mothers revealed that all 7 of their offspring exhibited SRV viremia, 6 of which were also antibody-negative. The present study demonstrates the occurrence of transplacental infection of SRV in viremic dams and infection of SRV in utero to induce immune tolerance in infant monkeys.

Abbreviation: SRV, simian betaretrovirus.

Although simian betaretrovirus (SRV) causes symptoms of immunodeficiency, including anemia, tumors, and persistent refractory diarrhea, in some infected macaques,[1,7,10] most infected monkeys exhibit few or no clinical signs.[2] Macaques free of SRV are important in many types of experiments to avoid associated immunologic and virologic effects. Establishing an SRV-free breeding colony is paramount for a steady supply of appropriate monkeys for various experiments.[8]

We previously reported that SRV-T, a novel subtype of SRV, was found in the cynomolgus colony of our institution.[3] Approximately 20% of the colony monkeys tested in 2005 were viremic and shed SRV-T virus in saliva, urine, and feces.[4,5] The viruses shed by these monkeys are a potential source of horizontal SRV-T infection, as occurred in a rhesus monkey colony.[6,7] In the present study, we investigated the actual prevalence and transmission of SRV in the closed cynomolgus colony through several generations, to prevent the spread of the virus and to establish an SRV-free colony.

Materials and Methods

Animals. The Tsukuba Primate Research Center (Tsukuba, Japan) maintains approximately 1500 cynomolgus monkeys as a breeding and rearing colony and has been maintained as a closed colony for 30 y. All adult monkeys are kept in single cages. Pregnant monkeys are produced by timed mating system in which a female monkey is placed into a male monkey's cage for 3 d; pregnancy is confirmed by ultrasonography 5 wk after mating.

Dams nurse their offspring until weaning at approximately 6 mo. Weaned infants are paired with infants of similar size. Artificial nursing is performed when the dams do not exhibit appropriate nursing behavior.

The housing and care procedures of this study were approved by the Animal Welfare and Animal Care Committee of Tsukuba Primate Research Center of the National Institute of Biomedical Innovation.

Samples. Blood samples were collected from 419 breeders (female, 364; male, 55). All of these monkeys were born at Tsukuba Primate Research Center and are the second and third generations from the founder monkeys, which originated from the Philippines, Malaysia and Indonesia.

We selected 95 pregnant monkeys that exhibited SRV-specific antibodies by Western blotting or the virus as detected by RT-PCR (or both) as the subjects of the study. Blood samples from the mothers and the newborn infant monkeys were collected within 12 h after parturition.

Western blotting. SRV-specific Abs were assessed by Western blotting using SRV-T.[5] Purified virus for this analysis was obtained from the culture supernatant of cloned SRV-T–infected A549 cells by ultracentrifugation through a sucrose gradient; purified viruses were disrupted by 1% SDS for use as antigen in Western blotting. The criterion for a positive reaction was detection of 2 or more virion-specific bands (that is, Gag and Env proteins).

RT-PCR. RNA was extracted from serum of the monkeys (QIAamp Viral RNA Mini Kit, Qiagen, Tokyo, Japan, or MagNA Pure Compact Nucleic Acid Isolation Kit I, Roche, Mannheim,

Received: 31 Jul 2009. Revision requested: 05 Sep 2009. Accepted: 11 Oct 2009.
[1]The Corporation for Production and Research of Laboratory Primates and [2]Tsukuba Primate Research Center (TPRC), National Institute of Biomedical Innovation, Tsukuba, Japan.
[*]Corresponding author. Email: fujimoto@primate.or.jp

Germany). Reverse transcription was performed (ThermoScript RT-PCR System, Invitrogen, Tokyo, Japan) by using gene-specific reverse primers. PCR analysis was performed (Premix Ex*Taq* Hot-Start Version, Takara, Shiga, Japan) by using published sets of external primers (SRVenv1E and SRVenv2E) and nested primers (SRVenv3N and SRVenv4N).[9]

Results

SRV infection status of the 419 laboratory-bred breeders. Of the 419 (female, 364; male, 55) cynomolgus macaques evaluated, 22 were negative for both SRV-specific antibodies and RNA. Of the remaining 397 breeders, 340 were positive for SRV-specific antibodies but were not viremic, 29 were positive for both viral RNA and antibodies, and the remaining 28 monkeys had viremia without antibodies.

SRV infection status of 95 pairs of mothers and offspring at birth. RT-PCR and Western blotting of samples from 95 pairs of mothers and offspring at the time of birth revealed that the dams could be grouped into 1 of 3 categories based on the presence of SRV-specific antibodies and viremia.[2] Among the 95 dams, 76 developed SRV-specific Abs without viremia, 14 had both antibodies and viremia, and the remaining 5 were viremic without SRV-specific antibodies.

None of the offspring of the 76 dams that were antibody-positive but RNA-negative were viremic at birth. Eight infants (including 2 delivered by caesarian section) of the 14 dually positive dams were viremic at birth; the remaining 6 infants of dams in this group were viral RNA-negative. All 5 progeny (including 2 infants delivered by caesarian section) of viremic but antibody-negative dams were viremic at birth.

Plasma SRV-specific antibodies and RNA in viremic newborns during the first 6 mo. We then tested the SRV-specific antibody and RNA status of 3 representative viremic newborns at 1, 2, and 6 mo after birth (Table 1). All 3 of the dams exhibited SRV viremia at delivery, and 2 of them also were positive for SRV-specific antibodies. All 3 infants exhibited SRV-specific RNA at all time points, but none was antibody-positive at weaning.

Family analysis of two representative SRV-viremic dams. The SRV status of all 7 offspring born to 2 representative viremic mothers was verified in 2007. Dam 1319711082 and her 4 offspring (infant 1410311011, born 2003; infant 1420506016, born 2005; infant 1420608031, born 2006; and infant 1420709050, born 2007) all demonstrated SRV RNA in tests performed during 2007. In addition, this dam and her oldest infant (1410311011) were antibody-positive, unlike the 3 youngest siblings. Dam 1319710076 and her 3 offspring (infant 1410408017, born 2004; infant 1410508022, born 2005; and infant 1420701001, born 2007) were all RNA-positive but antibody-negative according to tests performed in 2007.

Discussion

In 2005, we reported that about 20% of the cynomolgus monkeys in the colony at our institution exhibited SRV-T viremia and that virus was present in saliva, urine, and feces from the viremic monkeys.[3-5] Because the virus secreted from these monkeys was a potential source of horizontal SRV-T infection, we performed the current large-scale survey of SRV infections in our laboratory-bred monkeys and assessed the transmission of SRV through the generations represented in the colony.

The present study validated our concerns about vertical and horizontal SRV infections in the colony, because more than 90% of the laboratory-born breeders were positive for SRV-specific antibodies or virus (or both). The rate of viremia in the present study (14%) was smaller than that (20%) in the earlier survey,[5] which involved 49 retired breeders. The rate of viremia in a colony may vary depending on the age distribution of animals and their countries of origin. In particular, we hypothesize that the 28 monkeys that exhibited SRV viremia without specific antibodies are immunotolerant to SRV because of being infected in utero, as is reported to occur in rhesus and pigtailed macaques.[7,12]

To evaluate transplacental maternal–infant transmission of SRV, we tested 95 pairs of mothers and newborns, including 4 infants delivered by caesarean section, by using SRV-specific RT-PCR. The results showed that all monkeys exhibiting SRV-specific antibodies without viremia produced newborns without viremia. However, the transplacental SRV infections observed in infants included 4 newborns delivered by cesarean section from viremic mothers. In pigtailed monkeys, SRV2 was detected in the tissues and amniotic fluid of fetuses and in the blood of newborns delivered from viremic mothers.[12] In other cynomolgus monkeys, SRV was transmitted through transfusion of blood from a viremic donor but not from a nonviremic donor.[13] These findings indicate that SRV viremia of the mother is essential to establishing transplacental infection of the fetus. However, the production of 6 SRV-negative newborns from 14 viremic dams with SRV-specific antibodies may indicate that these antibodies reduced the viral loads in the viremic mothers sufficiently to prevent transplacental infection with SRV. Further investigation to quantify SRV in blood and the occurrence of transplacental infections will resolve this question.

An important issue is whether SRV viremic newborns can convert to a nonviremic state after developing virus-specific antibodies. Three infants born from viremic mothers exhibited viremia, which was maintained at 1, 2, and 6 mo of age, with no antibodies at 6 mo of age. In addition, 7 offspring born from the representative 2 SRV-viremic mothers were all viremic, at ages of 6 mo to 4 y. Pigtailed monkey newborns infected transplacentally with SRV2 maintained a viremic state for 1 y without producing antibodies and harbored proviral DNA in many tissues.[11,12] A newborn rhesus monkey produced from a viremic mother was SRV1-positive within 24 h after birth and was antibody-negative for as long as 6 mo after birth.[7] These findings suggest that cynomolgus infants infected in utero with SRV and born from viremic mothers are immunologically tolerant to the virus and that they then become the source of SRV infection in the colony.

The cynomolgus monkey breeding colony at our institution has been maintained as SPF with regard to B virus, SVV, SIV, STLV1, and measles virus but not SRV. The cage system used during the first 25 y was a two-story type—monkeys were able to touch feces and urine of animals in adjacent cages. In addition, cages were washed with high-pressure water, perhaps helping to spread virus-contaminated waste and increasing the likelihood of horizontal infections. After redesigning the cage system to a single-story type that prevents monkeys from touching fecal and urine waste from another macaque, we anticipate that we will be able to establish an SRV-free colony by introducing SRV nonviremic monkeys into the breeding colony. Furthermore, elimination of viremic dams, which can become a source of transplacental infection, from the breeding colony is critical to establishing an

Table 1. SRV-specific antibodies and RNA in the plasma of viremic newborns during their first 6 mo

Infant ID	Method of delivery	Dam ID	Method of nursing	Status of dam at parturition		Status of infant at				
						0 d	1 mo	2 mo	Weaning (approximately 6 mo)	
				Antibodies	RNA	RNA	RNA	RNA	Antibodies	RNA
1310611144	Caesarean	1210003019	Artificial	+	+	+	+	+	–	+
1410508022	Natural	1319710076	Artificial	–	+	+	+	+	–	+
1420506016	Natural	1319711082	Maternal	+	+	+	+	+	–	+

Testing of infants for SRV-specific antibodies was delayed until weaning because transplacentally transferred maternal antibodies can persist at 2 mo of age.

SRV-free breeding colony. The establishment of an SRV-free cynomolgus breeding colony is paramount for supplying monkeys that are appropriate for many fields of investigation, including vaccine testing, gene therapeutics, organ transplantation, and infectious disease studies.

Acknowledgment

This work was supported by a grant from the Ministry of Health, Labor, and Welfare of Japan.

References

1. **Daniel MD, King NW, Letvin NL, Hunt RD, Sehgal PK, Desrosiers RC.** 1984. A new type D retrovirus isolated from macaques with an immunodeficiency syndrome. Science **223:**602–605.
2. **Guzman RE, Kerlin RL, Zimmerman TE.** 1999. Histologic lesions in cynomolgus monkeys (*Macaca fascicularis*) naturally infected with simian retrovirus type D: comparison of seropositive, virus-positive, and uninfected animals. Toxicol Pathol **27:**672–677.
3. **Hara M, Sato T, Kikuchi T, Nakajima N, Uda A, Fujimoto K, Baba T, Mukai R.** 2005. Isolation and characterization of new simian retrovirus type D subtype from monkeys at the Tsukuba Primate Center, Japan. Microbes Infect **7:**126–131.
4. **Hara M, Kikuchi T, Ono F, Takano J, Ageyama N, Fujimoto K, Terao K, Baba T, Mukai R.** 2005. Survey of captive cynomolgus macaques colonies for SRV/D infection using polymerase chain reaction assays. Comp Med **55:**145–149.
5. **Hara M, Kikuchi T, Sata T, Nakajima N, Ami Y, Sato Y, Tanaka K, Narita T, Ono F, Akari H, Terao K, Mukai R.** 2007. Detection of SRV/D shedding in body fluids of cynomolgus macaques and comparison of partial gp70 sequences in SRV/D-T isolate. Virus Genes **35:**281–288.
6. **Lerche NW, Osborn KG, Marx PA, Prahalada S, Maul DH, Lowenstine LJ, Munn RJ, Bryant ML, Henrickson RV, Arthur LO, Gilden RV, Barker CS, Hunter E, Gardner MB.** 1986. Inapprent carriers of simian acquired immune deficiency syndrome type D retrovirus and disease transmission with saliva. J Natl Cancer Inst **77:**489–496.
7. **Lerche NW, Marx PA, Osborn KG, Maul DH, Lowenstine LJ, Bleviss ML, Moody P, Henrickson RV, Gardner MB.** 1987. Natural history of endemic Type D retrovirus infection and acquired immune deficiency syndrome in group-housed rhesus monkeys. J Natl Cancer Inst **79:**847–854.
8. **Lerche NW, Yee JL, Jennings MB.** 1994. Establishing specific retrovirus-free breeding colonies of macaques: an approach to primary screening and surveillance. Lab Anim Sci **44:**217–221.
9. **Liska V, Lerche NW, Ruprecht RM.** 1997. Simultaneous detection of simian retrovirus type D serotype 1, 2 and 3 by polymerase chain reaction. AIDS Res Hum Retroviruses **13:**433–437.
10. **Marx PA, Maul DH, Osborn KG, Lerche NW, Moody P, Lowenstine LJ, Henrickson RV, Arthur LO, Gilden RV, Gravell M, London WT, Sever JL, Levy JA, Munn RJ, Gardner MB.** 1984. Simian AIDS: isolation of a type D retrovirus and transmission of the diseases. Science **223:**1083–1086.
11. **Moazed TC, Thouless ME.** 1993. Viral persistence of simian type D retrovirus (SRV2/W) in naturally infected pigtailed macaques (*Macaca nemestrina*). J Med Primatol **22:**382–389.
12. **Tsai CC, Follis KE, Snyder K, Windsor S, Thouless ME, Kuller L, Morton WR.** 1990. Maternal transmission of type D simian retrovirus (SRV/D) in pregnant macaques. J Med Primatol **19:**203–216.
13. **Wilkinson RC, Murrell CK, Guy R, Davis G, Hall JM, North DC, Rose NJ, Almond N.** 2003. Persistence and dissemination of simian retrovirus type 2 DNA in relation to viremia, seroresponse, and experimental transmissibility in *Macaca fascicularis*. J Virol **77:**10751–10759.

Reduced Replication Capacity of NL4-3 Recombinant Viruses Encoding Reverse Transcriptase–Integrase Sequences From HIV-1 Elite Controllers

Zabrina L. Brumme, PhD,†‡ Chun Li, BSc,‡§ Toshiyuki Miura, MD,‡‖ Jennifer Sela, BSc,‡ Pamela C. Rosato, BSc,‡ Chanson J. Brumme, BSc,†‡ Tristan J. Markle, BSc,* Eric Martin, BSc,*§§ Brian L. Block, BSc,‡ Alicja Trocha, DVM,‡ Carl M. Kadie, PhD,¶ Todd M. Allen, PhD,‡ Florencia Pereyra, MD,‡ David Heckerman, MD, PhD,¶ Bruce D. Walker, MD,‡# and Mark A. Brockman, PhD*§§†‡*

Background: Identifying viral and host determinants of HIV-1 elite control may help inform novel therapeutic and/or vaccination strategies. Previously, we observed decreased replication capacity in controller-derived viruses suggesting that fitness consequences of human leukocyte antigen (HLA) class I–associated escape mutations in Gag may contribute to this phenotype. This study examines whether similar functional defects occur in Pol proteins of elite controllers.

Methods: Recombinant NL4-3 viruses encoding plasma RNA-derived reverse transcriptase–integrase sequences from 58 elite controllers and 50 untreated chronic progressors were constructed, and replication capacity measured in vitro using a green fluorescent protein (GFP) reporter T-cell assay. Sequences were analyzed for drug resistance and HLA-associated viral polymorphisms.

Results: Controller-derived viruses displayed significantly lower replication capacity compared with those from progressors ($P < 0.0001$). Among controllers, the most attenuated viruses were generated from individuals expressing HLA-B*57 or B*51. In viruses from B*57+ progressors (n = 8), a significant inverse correlation was observed between B*57-associated reverse transcriptase–integrase escape mutations and replication capacity ($R = -0.89$; $P = 0.003$); a similar trend was observed in B*57+ controller-derived viruses (n = 20, $R = -0.36$; $P = 0.08$).

Conclusions: HIV-1 Pol function seemed to be compromised in elite controllers. As observed previously for Gag, HLA-associated immune pressure in Pol may contribute to viral attenuation and subsequent control of viremia.

Key Words: Cytotoxic T-lymphocyte, elite controller, HIV-1, HLA class I, immune escape, Pol, viral replication capacity

(*J Acquir Immune Defic Syndr* 2011;56:100–108)

Received for publication January 5, 2010; accepted September 23, 2010.

From the *Faculty of Health Sciences and §§Department of Molecular Biology and Biochemistry, Simon Fraser University, Burnaby BC, Canada; †British Columbia Centre for Excellence in HIV/AIDS, Vancouver BC, Canada; ‡Ragon Institute of MGH, MIT, and Harvard, Boston, MA; §Program of Biological Sciences in Dental Medicine, Harvard University, Cambridge, MA; ‖Division of Infectious Diseases Advanced Clinical Research Center, Institute of Medical Science, University of Tokyo, Tokyo, Japan; ¶Microsoft Research, Redmond WA; and #Howard Hughes Medical Institute, Chevy Chase, MD.

Supported in part by grants AI028568 and AI030914 from the NIAID-NIH, the Howard Hughes Medical Institute, the Harvard University Center for AIDS Research, the Bill and Melinda Gates Foundation, and a gift from the Mark and Lisa Schwartz Foundation (to B.D.W.), and an Operating Grant from the Canadian Institutes of Health Research (CIHR) and a Jim Gray Seed Grant from Microsoft Research (to M.A.B. and Z.L.B.). Z.L.B. is supported by a CIHR New Investigator Award. C.J.B. is supported by a NSERC Julie Payette Scholarship.

Presented in part as: Li C, Brumme ZL, Miura T, Rosato P, Sela J, Brumme CJ, Heckerman D, Pereyra F, Walker BD, Brockman MA. Reduced replication capacity of NL4-3 chimeric viruses encoding reverse transcriptase–integrase sequences from HIV-1 elite controllers. AIDS Vaccine. 2009. Abstract P09-11.

The authors Z.L.B., C.L. contributed equally.

The authors declare no conflicts of interest related to this study.

Correspondence to: Mark A. Brockman, PhD, Associate Professor, Molecular Biology and Biochemistry, Simon Fraser University, South Sciences Building, Room 7153, 8888 University Drive, Burnaby, BC, Canada V5A 1S6 (e-mail: mark_brockman@sfu.ca).

Supplemental digital content is available for this article. Direct URL citations appear in the printed text and are provided in the HTML and PDF versions this article on the journal's Web site (www.jaids.com).

Copyright © 2011 by Lippincott Williams & Wilkins

INTRODUCTION

Elite controllers are a rare group of HIV-1–infected individuals who spontaneously maintain plasma viremia below the limit of standard clinical detection (<50 viral RNA copies/mL) without antiviral therapy.[1] Elucidating the mechanisms responsible for this phenotype may reveal host and viral factors that may be modulated for prophylactic or therapeutic intervention.

HIV-1 replication capacity (RC) likely plays an important role in pathogenesis,[2,3] but its relevance to the elite controller phenotype remains unclear. Although a recent examination of a large number of elite controller-derived HIV sequences revealed no evidence of gross mutational defects, large insertions or deletions, nor shared ancestry,[4] virus function may nevertheless be compromised. Indeed, previous studies have reported lower RC in viruses isolated from viremic long-term nonprogressors compared with those from

Copyright © Lippincott Williams & Wilkins. Unauthorized reproduction of this article is prohibited.

chronically infected individuals,[2,3,5] and reduced entry efficiency has been observed for elite controller-derived envelopes compared with those from chronically infected individuals.[6]

Although RC is determined in large part by the founder virus acquired at transmission,[7,8] it can change over time as host and other selective pressures drive intrahost HIV-1 evolution.[9–11] In vitro fitness costs of HLA-restricted cytotoxic T-lymphocyte (CTL) escape mutations in Gag[12–17] and Nef[18] have been demonstrated, and evidence suggests that immune-mediated fitness defects may be relevant to the controller phenotype.[19,20] A recent case report described reduced RC of virus isolated from a B*27/B*57-expressing elite controller compared with the transmitted donor virus.[19] Furthermore, we have previously described reduced in vitro RC of recombinant viruses expressing Gag-Protease from elite controllers compared with progressors in chronic[20] and acute/early[21] infection, an observation attributable at least in part to immune selection.[20,22] A biologically relevant role for immune-mediated fitness defects is supported by relative early viremia control in individuals who acquire HIV-1 harboring escape mutations from donors expressing protective HLA alleles.[7,8] Moreover, evidence for sequential reductions in RC as a result of the accumulation of HLA-restricted CTL escape mutations has been reported in Gag.[16,23]

However, comparably little is known about the consequence of mutations outside of the *Gag* gene on viral RC in elite controllers, and what relevance this may have to the controller phenotype. Because mutations in the *Pol* gene that emerge under antiretroviral drug selection pressures can affect fitness,[24–28] we therefore examined whether elite controller viruses exhibited functional defects in this gene. To do this, recombinant viruses encoding plasma RNA-derived reverse transcriptase (RT)–integrase sequences were generated in an NL4-3 virus backbone from 58 elite controllers and 50 untreated chronic progressors and their in vitro RC was examined using a GFP reporter T-cell assay.[20,29] Similar to previous observations for Gag-Protease[20,21] and Envelope,[6] we observed reduced function of controller-derived RT–integrase, indicating that differences in Pol activity may contribute to HIV-1 control.

METHODS

Study Participants

Fifty-eight elite controllers {all <50 copies RNA/mL; median CD4 = 799 [interquartile range (IQR): 593–1037] cells/mm^3} and 50 untreated chronic progressors [median viral load 4.98 (IQR: 4.51–5.35) $\log_{10}$ copies RNA/ml; median CD4 = 318 (IQR: 61–476) cells/mm^3] were included. Characteristics of this elite controller cohort have been described previously.[30] In addition, 76 of these 108 (70%) patients were previously evaluated for Gag-Protease function.[20] HLA class I typing was performed using standard sequence-based methods. This study was approved by the institutional review board at Massachusetts General Hospital; written informed consent was obtained from all participants.

Generation of Recombinant RT–Integrase Viruses

Bulk (Quasispecies) Method

For elite controllers, reverse transcriptase–polymerase chain reaction (RT-PCR) products spanning Pol were generated as described.[4] For progressors, HIV-1 Pol was RT-PCR amplified from extracted plasma HIV RNA using sequence-specific primers. Second-round polymerase chain reaction (PCR) was performed using PAGE-purified "recombination primers" designed to match the NL4-3 sequence directly upstream of RT (forward; 100bp) and downstream of integrase (reverse; 98bp). Primer sequences are available upon request.

Plasmid pNL4-3ΔRT-Integrase was developed by inserting unique restriction enzyme sites for BstEII at the 5′ end of RT and the 3′ end of integrase using the QuikChange XL kit (Stratagene) followed by deletion of the intervening region by BstEII digestion (New England Biolabs, Ipswich, MA). This plasmid was maintained using Stbl3 E. coli cells (Invitrogen, Burlington, ON, Canada). To generate recombinant viruses, 10 μg of BstEII-linearized plasmid plus 50 μL of second-round amplicon (approximately 5 μg) were mixed with 2.0×10^6 cells of a Tat-driven GFP reporter T-cell line (GXR25 cells[29]) in 800 μL of R10+ medium (RPMI 1640 containing 10% FCS, 2 mM L-glutamine, 100 units/mL penicillin, and 100 μg/mL streptomycin), and transfected by electroporation using a BioRad GenePulser Xcell (exponential protocol: 300V, 500 μF). After transfection, cells were rested for 45 minutes at room temperature, transferred to 25 cm^2 flasks in 5 mL of R10+ medium, and fed with 5 mL R10+ medium on day 5. GFP expression was monitored daily by flow cytometry (FACScalibur, BD Biosciences) starting on day 10. Once GFP+ expression reached ~15% among viable cells, representing the early phase of exponential spread, culture supernatants containing the recombinant viruses were harvested and aliquots stored at −80°C.

Clonal Method

In addition, RT–integrase sequences from a random subset of 14 controllers and 10 progressors were cloned (TOPO-TA cloning kit; Invitrogen, Burlington, ON, Canada), purified and used as starting material to generate recombinant viruses as described above. All clones were resequenced to confirm patient origin.

RC Assays

Virus titers and replication assays were performed as described.[12,20,29] Replication assays were initiated at multiplicity of infection = 0.003, and included 6 negative (uninfected cells only) and 6 NL4-3 controls in each experiment. For each virus, the natural log of the slope of the percent of GFP+ cells was calculated during the exponential phase of viral spread in culture (days 3–6). This value was divided by the mean rate of spread of NL4-3 to generate a normalized, quantitative measure of RC. An RC of 1.0 indicates a rate of spread equal to NL4-3, whereas RC <1.0 and >1.0 indicate rates of spread that are slower than or faster than NL4-3, respectively. All assays were performed in triplicate in

© 2011 Lippincott Williams & Wilkins

Copyright © Lippincott Williams & Wilkins. Unauthorized reproduction of this article is prohibited.